Reactivity of the Heterobinuclear Phenylacetylide-Bridged A-Frame $[RhIr(CO)_2(\mu\text{-}CCPh)(Ph_2PCH_2PPh_2)_2][O_3SCF_3]$ with Small Molecules

Darren S. A. George, Robert McDonald,† and Martin Cowie*

Department of Chemistry, University of Alberta, Edmonton, AB, Canada T6G 2G2

Received October 30, 1997

The compound $[RhIr(CO)_2(\mu\text{-}CCPh)(dppm)_2][O_3SCF_3]$ (**2**, dppm = $Ph_2PCH_2PPh_2$) is an "A-frame" species in which the bridging phenylacetylide group is σ-bound to iridium and functioning as a π donor to rhodium. Compound **2** reacts with CO and SO_2 to give the carbonyl- and sulfur dioxide-bridged products $[RhIr(CO)_2(\mu\text{-}CCPh)(\mu\text{-}L)(dppm)_2][O_3SCF_3]$ (L = CO (**1**), SO_2 (**5**)), respectively. Reaction of **2** with a hydride source yields $[RhIr(H)(CO)_2(\mu\text{-}CCPh)(dppm)_2]$ (**6**), having the hydride terminally bound to iridium, and this product rearranges at room temperature to give the phenylvinylidene complex $[RhIr(CO)_2(\mu\text{-}CC(H)Ph)(dppm)_2]$ (**7**). Phosphines, olefins, and alkynes also bind terminally to iridium, yielding $[RhIr(L)(CO)_2(\mu\text{-}CCPh)(dppm)_2][O_3SCF_3]$ (L = PR_3, olefin, alkyne). In the case of dimethyl acetylenedicarboxylate, rearrangement of the initial alkyne adduct occurs to give the alkyne-bridged product $[RhIr(CO)_2(\mu\text{-}CCPh)(\mu\text{-}CH_3O_2CC{\equiv}CCO_2CH_3)(dppm)_2][O_3SCF_3]$ (**18**). In addition, the initial adducts of terminal alkynes also rearrange by an oxidative addition reaction to give the bis(acetylide) hydride species $[RhIr(CCPh)(CO)_2(\mu\text{-}H)(\mu\text{-}CCR)(dppm)_2][O_3SCF_3]$ (R = Ph (**19**), CH_3 (**20**)). Compound **2** also undergoes oxidative addition with dihydrogen to give $[RhIr(H)(CO)_2(\mu\text{-}H)(\mu\text{-}CCPh)(dppm)_2][O_3SCF_3]$ (**21**), in which the terminal (on Ir) and the bridging hydrides are in the A-frame pocket. It appears that SO_2 and H_2 attack on the inside of the A-frame pocket, whereas all other substrates attack on the outside of the pocket, at iridium.

Introduction

Our understanding of organometallic processes, particularly involving late transition metals, in both stoichiometric and catalytic reactions, has benefited greatly from studies of d^8, square planar complexes such as $RhCl(PPh_3)_3$ and $IrCl(CO)(PPh_3)_2$.[1] One series of analogous complexes, in which the chloro ligand is replaced by an anionic organic group, such as an alkyl, aryl, or related group, presents an interesting extension to the chemistry. Not only can the electronic influence of this group give rise to interesting reactivity changes at the metal,[1g,2] but C−C bond formation is also possible through migratory insertion reactions involving carbon-containing substrates and the anionic, organic ligand.[3]

Our interest in the above systems, involving ligands such as alkyl, aryl, and alkenyl groups,[4] has centered on binuclear complexes in which the adjacent metals can somehow interact in a cooperative manner when activating organic substrates. Binuclear complexes of this type are members of the so-called "A-frame"[5] series, in which the metals are bridged by a single ligand in addition to the diphosphine groups, which are mutually trans on each metal.

We have recently begun an investigation of binuclear complexes containing the acetylide or alkynyl ligand (−C≡CR), for which a variety of organic transformations has been demonstrated, including cycloaddition,[6] carbon−

* To whom correspondence should be addressed. Fax: (403)-492-8231. E-mail: martin.cowie@ualberta.ca.

† Faculty Service Officer, Structure Determination Laboratory.

(1) (a) Collman, J. P.; Hegedus, L. S.; Norton, J. R.; Finke, R. G. *Principles and Applications of Organotransition Metal Chemistry*; University Science Books: Mill Valley, CA, 1987. (b) Jardine, F. H.; Osborn, J. A.; Wilkinson, G. *J. Chem. Soc. A* **1967**, 1574. (c) Collman, J. P. *Acc. Chem. Res.* **1968**, *1*, 136. (d) Collman, J. P. *Adv. Organomet. Chem.* **1968**, *7*, 53. (e) Vaska, L. *Acc. Chem. Res.* **1968**, *1*, 335. (f) Halpern, J. *Inorg. Chim. Acta* **1981**, *50*, 11. (g) Atwood, J. D. *Coord. Chem. Rev.* **1988**, *83*, 93.

(2) Rees, W. M.; Churchill, M. R.; Li, Y.-J.; Atwood, J. D. *Organometallics* **1985**, *4*, 1162. (b) Walter, R. H.; Johnson, B. F. G. *J. Chem. Soc., Dalton Trans.* **1978**, 381.

(3) (a) Kein, W. *J. Organomet. Chem.* **1969**, *19*, 161. (b) English, A. D.; Herskovitz, J. *J. Am. Chem. Soc.* **1977**, *99*, 1648. (c) Calabrese, J. C.; Roe, D. C.; Thorn, D. L.; Tulip, T. H. *Organometallics* **1984**, *3*, 1223. (d) Darensbourg, D. J.; Grötsch, G.; Wiegreffe, P.; Rheingold, A. L. *Inorg. Chem.* **1987**, *26*, 3827. (e) Kramarz, K. W.; Eisenschmid, T. C.; Deutsch, D. A.; Eisenberg, R. *J. Am. Chem. Soc.* **1991**, *113*, 5090. (f) Foo, T.; Bergman, R. G. *Organometallics* **1992**, *11*, 1811. (g) Kramarz, K. W.; Eisenberg, R. *Organometallics* **1992**, *11*, 1997. (h) Cleary, B. P.; Eisenberg, R. *Organometallics* **1992**, *11*, 2335. (i) Shafiq, F.; Kramarz, K. W.; Eisenberg, R. *Inorg. Chim. Acta* **1993**, *213*, 111.

(4) (a) Antonelli, D. M.; Cowie, M. *Organometallics* **1991**, *10*, 2550. (b) Antwi-Nsiah, F. R.; Cowie, M. *Organometallics* **1992**, *11*, 3157. (c) Sterenberg, B. T.; Hilts, R. W.; Moro, G.; McDonald, R.; Cowie, M. *J. Am. Chem. Soc.* **1995**, *117*, 245. (d) Wang, L.-S.; Cowie, M. *Organometallics* **1995**, *14*, 2374. (e) Wang, L.-S.; Cowie, M. *Organometallics* **1995**, *14*, 3040. (f) Wang, L.-S.; Cowie, M. *Can. J. Chem.* **1995**, *73*, 1058. (g) Antwi-Nsiah, F. H.; Oke, O.; Cowie, M. *Organometallics* **1996**, *15*, 506. (h) Antwi-Nsiah, F. H.; Oke, O.; Cowie, M. *Organometallics* **1996**, *15*, 1042. (i) Sterenberg, B. T.; Cowie, M. *Organometallics* **1997**, *16*, 2297. (j) Graham, T. W.; Van Gastel, F.; Cowie, M. Manuscript in preparation. (k) Torkelson, J. R.; Antwi-Nsiah, F. H.; Cowie, M.; Pruis, J. G.; Jalkanen, K. J.; DeKock, R. Manuscript in preparation. (m) Oke, O.; Cowie, M. Manuscript in preparation.

(5) Kubiak, C. P.; Eisenberg, R. *J. Am. Chem. Soc.* **1977**, *99*, 6129.

S0276-7333(97)00946-1 CCC: $15.00
Publication on Web 05/16/1998

carbon bond formation,[7] and transformations to vinylidenes[8]—themselves useful precursors for further organic transformations.[9] The alkynyl ligand is isoelectronic with the carbonyl group and displays some of the same structural diversity[10] of this ubiquitous group. At a single metal center the alkynyl group binds in an η^1-fashion through the terminal carbon, whereas in multinuclear systems a number of bridging modes are possible. The common modes observed in a heterobinuclear system (M ≠ M′) are diagrammed as follows:

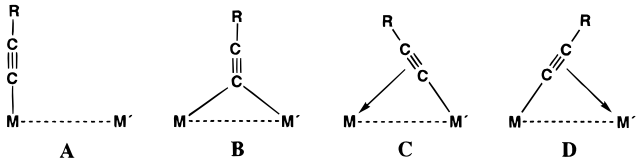

In structure **A**, the alkynyl group is terminally bound to either metal M or M′ and, to a first approximation, resembles a mononuclear system. The direct involvement of the second metal can occur as shown in the other modes. In structure **B**, the alkynyl group functions as a two-electron donor to the pair of metals, much as in a symmetrically bridging carbonyl. When the alkynyl group functions as an asymmetric bridge, as in **C** or **D**, it behaves as a two-electron donor to one metal, via the M−C σ bond, and as a two-electron donor to the other, via the π-interaction. However, the above structural analogy between −C≡CR and CO should not be extended too far into electronic effects, since it is generally accepted that, unlike carbonyls, the alkynyl group has very poor π-acceptor capabilities in the η^1-binding mode.[11]

In this paper we present the first of our studies on the chemistry of the phenylacetylide-bridged compound $[RhIr(CO)_2(\mu\text{-}CCPh)(dppm)_2][O_3SCF_3]$ (**2**), in which we concentrate on determining the roles of the different metals in the reactivity of this species.

Experimental Section

All solvents were distilled over appropriate drying agents (sodium/benzophenone for THF, ether, benzene, and pentane; phosphorus pentoxide for halogenated solvents) before use. Reactions were done at ambient temperature using standard Schlenk techniques (under either dinitrogen or argon) unless otherwise stated. Prepurified dinitrogen, argon, and carbon monoxide were purchased from Praxair Products, Inc., allene was obtained from Canadian Liquid Air Ltd., and dihydrogen was purchased from Linde. All gases were used as received. Ammonium hexachloroiridate(IV) and potassium hexachlororhodate(III) were obtained from Vancouver Island Precious Metals; hydrated rhodium trichloride was purchased from Colonial Metals. The compounds $[IrAgCl(CCPh)(CO)(dppm)_2]$,[12] $[Rh_2(CO)_4Cl_2]$,[13] and $[Rh_2(COD)_2Cl_2]$[14] were prepared by literature methods. Dimethyl acetylenedicarboxylate (DMAD, obtained from Aldrich) and deuterated solvents (obtained from Cambridge Isotope Laboratories) were distilled and stored over molecular sieves. The previously reported[4g] compound $[RhIr(CO)_3(CCPh)(dppm)_2]Cl$ (**1**) was prepared by a variation on Shaw's method,[12] as outlined below. All other reagents were obtained from Aldrich and were used as received.

NMR spectra were obtained on either a Bruker 400 MHz spectrometer (operating at 100.614 MHz for ^{13}C, 161.978 MHz for ^{31}P, and 376.503 MHz for ^{19}F) or a Bruker 200 MHz spectrometer (operating at 50.323 MHz for ^{13}C and 81.015 MHz for ^{31}P). Infrared spectra were run on either a Perkin-Elmer model 1600 FTIR or a Nicolet Magna-IR 750 spectrometer as either solids (Nujol mulls on KBr disks) or solutions (KCl cell with 0.5 mm window path length). Elemental analyses were conducted by the microanalytical service within the department. Spectroscopic data for all compounds is given in Table 1.

(a) Preparation of $[RhIr(CO)_3(\mu\text{-}\eta^1\text{:}\eta^{2'}\text{-}CCPh)(dppm)_2]Cl$ (1). A solid sample of $[IrAgCl(CO)(CCPh)(dppm)_2]$ (198.5 mg, 160.9 μmol) was placed in a flask with $[Rh_2(CO)_4Cl_2]$ (33 mg, 84.9 μmol) and 10 mL of CH_2Cl_2. The solution was stirred for $^1/_2$ h, during which time it changed from a red solution to a brown suspension. Filtration resulted in a clear red solution. The solvent was reduced to 2 mL under a stream of CO, and the product precipitated by the addition of 20 mL of ether. The resulting brown precipitate was then washed twice with 10 mL of ether and dried under nitrogen. It was shown by its proton and phosphorus NMR spectra to be analogous to the previously reported triflate salt.[4g] Yield: 193 mg (93%).

(b) Preparation of $[RhIr(CO)_2(\mu\text{-}\eta^1\text{:}\eta^{2'}\text{-}CCPh)(dppm)_2][O_3SCF_3]$ (2). (Method 1). A solid sample of $[IrAgCl(CO)(CCPh)(dppm)_2]$ (0.97 g, 789.4 μmol) was placed in a flask with $[Rh_2(CO)_4Cl_2]$ (154 mg, 396.1 μmol) and 60 mL of CH_2Cl_2, yielding a brown-red mixture which was stirred for $^1/_2$ h, followed by addition of 5 mL of a THF solution of AgO_3SCF_3 (215 mg, 836 μmol) via cannula. The solution was filtered after a further 30 min of stirring, and then the solvent was removed in vacuo. The resulting solid was dissolved in 5 mL of CH_2Cl_2 and 20 mL of THF, and the solution was refluxed for 2 h. The solvent was reduced to 10 mL, and the product was precipitated by the addition of ether (60 mL). The red product was then washed three times with 10 mL aliquots of ether. Yield: 0.97 g (90%). Calcd for $C_{61}H_{49}O_5P_4RhIrF_3S$: C, 53.47; H, 3.60. Found: C, 53.72; H, 3.58.

Method 2. A solid sample of $[IrAgCl(CO)(CCPh)(dppm)_2]$ (1.50 g, 1.22 mmol) was placed in a flask with $[Rh_2(COD)_2Cl_2]$ (267 mg, 608.1 μmol) and 30 mL of CH_2Cl_2. The resulting brown-red mixture was stirred for 1 h, and then an atmosphere of CO was placed over the solution. After a further 15 min of stirring, 5 mL of a THF solution of AgO_3SCF_3 (310 mg, 1.207 mmol) was added via cannula. The solution was filtered after a further 30 min of stirring, and then the solvent was removed

(6) Bruce, M. I.; Hambley, T. W.; Liddell, M. J.; Snow, M. R.; Swincer, A. G.; Tiekink, E. R. T. *Organometallics* **1990**, *9*, 96. (b) Barrett, A. G. M.; Carpenter, N. E.; Mortier, J.; Sabat, M. *Organometallics* **1990**, *9*, 151. (c) Bruce, M. I.; Duffy, D. N.; Liddell, M. J.; Tiekink, E. R. T.; Nicholson, B. K. *Organometallics* **1992**, *11*, 1527. (d) Fischer, H.; Leroux, F.; Roth, G.; Stumpf, R. *Chem. Ber.* **1996**, *129*, 1475. (e) Fischer, H.; Leroux, F.; Roth, G.; Stumpf, R. *Organometallics* **1996**, *15*, 3723.

(7) McMullen, A. K.; Selegue, J. P.; Wang, J.-G. *Organometallics* **1991**, *10*, 3421. (b) Matsuzaka, H.; Hirayama, Y.; Nishio, M.; Mizobe, Y.; Hidai, M. *Organometallics* **1993**, *12*, 36. (c) Barbaro, P.; Bianchini, C.; Peruzzini, M.; Polo, A.; Zanobini, F.; Frediani, P. *Inorg. Chim. Acta* **1994**, *220*, 5. (d) Bianchini, C.; Frediani, P.; Masi, D.; Peruzzini, M.; Zanobini, F. *Organometallics* **1994**, *13*, 4616. (e) Werner, H.; Schäfer, M.; Wolf, J.; Peters, K.; von Schnering, H. G. *Angew. Chem., Int. Ed. Engl.* **1995**, *34*, 191. (f) Albertin, G.; Antoniutti, S.; Bordignon, E.; Cazzaro, F.; Ianelli, S.; Pelizzi, G. *Organometallics* **1995**, *14*, 4114. (g) Yamamoto, Y.; Satoh, R.; Tanase, T. *J. Chem. Soc., Dalton Trans.* **1995**, 307. (h) Klein, H.-F.; Heiden, M.; He, M.; Jung, T.; Röhr, C. *Organometallics* **1997**, *16*, 2003.

(8) (a) Elschenbroich, Ch.; Salzer, A. *Organometallics: A Concise Introduction*; VCH Publishers: New York, 1989. (b) Esteruelas, M. A.; Lahoz, F. J.; Oñate, E.; Oro, L. A.; Rodríguez, L. *Organometallics* **1993**, *12*, 4219. (c) Werner, H. *J. Organomet. Chem.* **1994**, *475*, 45. (d) Edwards, A. J.; Esteruelas, M. A.; Lahoz, F. J.; Modrego, J.; Oro, L. A.; Schrickel, J. *Organometallics* **1996**, *15*, 3556.

(9) Bruce, M. I. *Chem. Rev.* **1991**, *91*, 197.

(10) (a) Nast, R. *Coord. Chem. Rev.* **1982**, *47*, 89. (b) Lotz, S.; van Rooyen, P. H.; Meyer, R. *Adv. Organomet. Chem.* **1995**, *37*, 219.

(11) (a) Lichtenberger, D. L.; Renshaw, S. K.; Bullock, R. M. *J. Am. Chem. Soc.* **1993**, *115*, 3276. (b) Manna, J.; John, K. D.; Hopkins, M. D. *Adv. Organomet. Chem.* **1995**, *38*, 79.

(12) Hutton, A. T.; Pringle, P. G.; Shaw, B. L. *Organometallics* **1983**, *2*, 1889.

(13) McCleverty, J. A.; Wilkinson, G. *Inorg. Synth.* **1990**, *28*, 85.

(14) Giordano, G.; Crabtree, R. H. *Inorg. Synth.* **1990**, *28*, 88.

Table 1. Spectral Data[a]

compd	NMR $\delta(^{31}P\{^1H\})$[b]	NMR $\delta(^{13}C\{^1H\})$[c]	NMR $\delta(^1H)$[c]	IR, cm^{-1} [d]
$[RhIr(CO)_2(CCPh)(dppm)_2][O_3SCF_3]$ (**2**)	21.0 (dm, $^1J_{RhP}$ = 110.5 Hz), 6.85 (m)	185.2 (dt, Rh−*C*O, $^2J_{PC}$ = 15.6 Hz, $^1J_{RhC}$ = 81.1 Hz), 185.0 (t, Ir−*C*O, $^2J_{PC}$ = 10.8 Hz), 107.9 (dtt, Ir−*C*≡CPh, $^2J_{P(Ir)C}$ = 14.7 Hz, $^1J_{RhC}$ = 5.1 Hz, $^2J_{P(Rh)C}$ = 4.7 Hz), 106.0 (dt, Ir−C≡*C* Ph, $^1J_{RhC}$ = 5.7 Hz, $^2J_{PC}$ ≈ 2 Hz)	3.8 (2H, m), 4.25 (2H, m)	1973 (s), 2025 (w)[k]
$[RhIr(CO)_2(PMe_3)(CCPh)(dppm)_2]$-$[O_3SCF_3]$ (**3**)	14.4 (dm, 2P, $^1J_{RhP}$ = 114.8 Hz), −25.8 (m, 2P), −63.3 (m, 1P)		5.1 (2H, m), 4.65 (2H, m), 0.7 (9H, d)	1935 (s), 1962 (m)
$[RhIr(CO)_2(PPhMe_2)(CCPh)(dppm)_2]$-$[O_3SCF_3]$ (**4**)	17.9 (ddm, 2P, $^1J_{RhP}$ = 114.2 Hz $^XJ_{PP}$ = 6.3 Hz), −23.1 (m, 2P), −55.4 (dtt, 1P, $^2J_{PP}$ = 24.2 Hz $^XJ_{PP}$ = 6.3 Hz $^XJ_{RhP}$ ≈ 7 Hz)	192.0 (ddt, Rh−*C*O, $^2J_{P(Rh)C}$ = 17.1 Hz, $^1J_{RhC}$ = 75.9 Hz, $^XJ_{P(PR3)C}$ = 4.4 Hz) 185.5 (t, Ir−*C*O, $^2J_{PC}$ = 12.3 Hz), 99.9 (m, Ir−*C*≡CPh), 90.3 (m, Ir−C≡*C*Ph), 16.7 (d, P*C*H_3, $^1J_{PC}$ = 26.8 Hz)	4.6 (2H, m), 4.1 (2H, m), 1.2 (6H, d)	1939 (s), 1973 (m)
$[RhIr(CO)_2(\mu\text{-}SO_2)(CCPh)(dppm)_2]$-$[O_3SCF_3]$ (**5**)	27.3 (dm, $^1J_{RhP}$ = 88.0 Hz), −7.1 (m)	188.4 (dt, Rh−*C*O, $^2J_{PC}$ = 16.4 Hz, $^1J_{RhC}$ = 64.4 Hz), 177.1 (t, Ir−*C*O, $^2J_{PC}$ = 11.6 Hz), 122.9 (t, Ir−*C*≡CPh, $^2J_{PC}$ = 1.9 Hz), 117.5 (dt, Ir−C≡*C*Ph, $^1J_{RhC}$ = 5.2 Hz, $^2J_{PC}$ = 3.1 Hz)	3.8 (4H, m)	1995 (s), 1964 (s), 1213 (w)[m], 1174 (w)[m], 1063 (m)[m], 1042 (m)[m]
$[RhIr(CO)_2(H)(CCPh)(dppm)_2]$ (**6a**)[g,j]	25.2 (dm, $^1J_{RhP}$ = 140.8 Hz), −3.4 (m)	191.7 (dt, Rh−*C*O, $^2J_{PC}$ = 16.6 Hz, $^1J_{RhC}$ = 73.6 Hz), 187.4 (t, Ir−*C*O, $^2J_{PC}$ = 7.4 Hz)	4.9 (2H, m), 4.25 (2H, m), −8.72 (t, $^2J_{PH}$ = 9.2 Hz)	
$[RhIr(CO)_2(H)(CCPh)(dppm)_2]$ (**6b**)[e,j]	14.0 (b), −17.5 (m)	186.1 (dm, $^1J_{RhC}$ = 67.3 Hz), 175.9 (b)	5.7 (2H, m), 5.0 (2H, m), −11.8 (t,$^2J_{PH}$ = 13.1 Hz)	
6b[h,j]	16.2 (dm, $^2J_{PP}$ ≈ 350 Hz), 6.4 (dm, $^2J_{PP}$ ≈ 350 Hz), −16.9 (dm, $^2J_{PP}$ ≈ 365 Hz), −22.9 (dm, $^2J_{PP}$ ≈ 365 Hz)		5.3 (2H, b), 4.9 (2H, b), −12.2 (b)	
$[RhIr(CO)_2(\mu\text{-}CCHPh)(dppm)_2]$ (**7a**)[j]	26.8 (dm, $^1J_{RhP}$ = 154.0 Hz), 18.2 (m)	198.8 (dt, Rh−*C*O, $^2J_{PC}$ = 15.2 Hz, $^1J_{RhC}$ = 59.1 Hz), 199.4 (t, Ir−*C*O, $^2J_{PC}$ = 8.9 Hz), 249.8 (dt, μ-*C*=CHPh, $^2J_{PC}$ = 12.8 Hz, $^1J_{RhC}$ = 19.6 Hz)	3.8 (2H, m), 3.05 (2H, m)	1943, 1914
$[RhIr(CO)_2(\mu\text{-}CCHPh)(dppm)_2]$ (**7b**)[j]	28.5 (dm, $^1J_{RhP}$ = 165.8 Hz), 15.9 (m)	202.6 (dt, Rh−*C*O, $^2J_{PC}$ = 13.1 Hz, $^1J_{RhC}$ = 60.5 Hz), 196.3 (t, Ir−*C*O, $^2J_{PC}$ = 11.0 Hz), 246.5 (dt, μ-*C*=CHPh, $^2J_{PC}$ = 11.8 Hz, $^1J_{RhC}$ = 17.0 Hz)	3.8 (2H, m), 2.7 (2H, m)	1943, 1914
$[RhIr(CO)_2(CH_2CH_2)(CCPh)(dppm)_2]$-$[O_3SCF_3]$ (**8**)[h]	20.65 (dm, $^1J_{RhP}$ = 105 Hz), −9.3 (m)	193.3 (dt, Rh−*C*O, $^2J_{PC}$ = 16.5 Hz, $^1J_{RhC}$ = 80.4 Hz),[i] 186.9 (b, Ir−*C*O)[i]	4.06 (2H, m), 3.27 (2H, m), 1.4 (2H, b), 0.75 (2H, b)	
$[RhIr(CO)_2(\eta^2\text{-}CH_2CCH_2)(CCPh)(dppm)_2]$-$[O_3SCF_3]$ (**9a**)[e]	20.7 (dm, $^1J_{RhP}$ = 104.8 Hz), −14.4 (m)	193.1 (dt, Rh−*C*O, $^2J_{PC}$ = 16.6 Hz, $^1J_{RhC}$ = 80.0 Hz), 186.9 (dt, Ir−*C*O, $^2J_{PC}$ ≈ $^1J_{RhC}$ ≈ 5 Hz)	6.1 (1H, s), 5.65 (1H, s), 4.15 (2H, m), 3.35 (2H, m), 0.30 (2H, b)	
$[RhIr(CO)_2(\eta^2\text{-}CH_2CCH_2)(CCPh)(dppm)_2]$-$[O_3SCF_3]$ (**9b**)[e]	21.9 (dm, $^1J_{RhP}$ = 101.1 Hz), −8.7 (m)	193.8 (dt, Rh−*C*O, $^2J_{PC}$ = 16.7 Hz, $^1J_{RhC}$ = 78.5 Hz), 191.9 (b, Ir−*C*O)	5.4 (1H, s), 4.4 (1H, s), 4.0 (2H, m), 3.2 (2H, m), 1.2 (2H, b)	
$[RhIr(CO)_2(\eta^2\text{-}CH_2CC(CH_3)_2)$-$(CCPh)(dppm)_2][O_3SCF_3]$ (**10**)	21.3 (dm, $^1J_{RhP}$ = 104.0 Hz), −12.5 (m)	193.6 (dt, Rh−*C*O, $^2J_{PC}$ = 16.5 Hz, $^1J_{RhC}$ = 79.9 Hz), 189.1 (dt, Ir−*C*O, $^2J_{PC}$ = 7.8 Hz, $^1J_{RhC}$ = 6.3 Hz), 76.4 (dtt, Ir−*C*≡CPh, $^2J_{P(Ir)C}$ = 9.9 Hz, $^1J_{RhC}$ = 9.0 Hz, $^2J_{P(Rh)C}$ = 2.2 Hz), 107.6 (d, Ir−C≡*C*Ph, $^1J_{RhC}$ = 3.6 Hz), 118.0 (t, =*C*$(CH_3)_2$, $^2J_{PC}$ = 3.4 Hz), 144.8 (t, CH_2=*C*=, $^2J_{PC}$ = 6.6 Hz), 25.1, 25.2 (s, =C(*C*H_3)$_2$), −6.4 (s, *C*H_2=C=)	4.1 (2H, m), 3.3 (2H, m), 1.80 (2H, b), 1.4 (3H, s), 0.7 (3H, s)	1964 (s), 1882 (b)

[RhIr(CO)$_2$(η^2-CF$_3$C≡CCF$_3$)(CCPh)(dppm)$_2$]-[O$_3$SCF$_3$] (**11**)	20.0 (dm, $^1J_{RhP}$ = 102.0 Hz), −10.6 (m)	192.1 (dt, Rh−*C*O, $^2J_{PC}$ = 16.3 Hz, $^1J_{RhC}$ = 81.0 Hz), 184.7 (m, Ir−*C*O, $^2J_{PC}$ = 7.5 Hz, $^1J_{RhC}$ = 10.0 Hz $^4J_{CF}$ = 3.5 Hz), 67.2 (m, Ir−*C*≡CPh, $^2J_{PC} \approx {}^1J_{RhC} \approx$ 8 Hz), 109.9 (d, Ir−C≡*C*Ph, $^1J_{RhC}$ = 3.0 Hz), 92.9 (qm, CF$_3$*C*≡CCF$_3$, $^2J_{CF} \approx$ 37 Hz, $^2J_{PC}$ = 4.7 Hz), 89.1 (qm, CF$_3$C≡*C*CF$_3$, $^2J_{CF} \approx$ 43 Hz), 119.3 (q, *C*F$_3$C≡, $^1J_{CF}$ = 269.6 Hz), 117.2 (q, *C*F$_3$C≡, $^1J_{CF}$ = 270.3 Hz)	4.2 (2H, m), 3.3 (2H, m)	1992 (s), 1865 (m), 1770 (m)[k]
[RhIr(CO)$_2$(η^2-CH$_3$OC(O)C≡CCO$_2$CH$_3$)-(CCPh)(dppm)$_2$][O$_3$SCF$_3$] (**12**)	21.7 (dm, $^1J_{RhP}$ = 102.7 Hz), −10.3 (m)	192.8 (dt, Rh−*C*O, $^2J_{PC}$ = 16.1 Hz, $^1J_{RhC}$ = 81.0 Hz), 185.2 (dt, Ir−*C*O, $^2J_{PC} \approx {}^1J_{RhC} \approx$ 7.2 Hz)	4.2 (2H, m), 3.2 (2H, m), 3.7 (3H, s), 3.0 (3H, s)	1983(s), 1878(b), 1779(m)[k], 1695(m)[l]
[RhIr(CO)$_2$(η^2-CH$_3$C≡CCO$_2$CH$_2$CH$_3$)-(CCPh)(dppm)$_2$][O$_3$SCF$_3$] (**13**)[f]	22.0 (dm, $^1J_{RhP}$ = 100.0 Hz), −13.0 (m)	195.2 (dt, Rh−*C*O, $^2J_{PC}$ = 15.3 Hz, $^1J_{RhC}$ = 81.5 Hz),[h] 189.7 (b, Ir−*C*O, $^1J_{RhC}$ = 12.6 Hz)[h]	4.15 (2H, m), 3.0 (2H, m), 4.15 (2H, q), 1.3 (3H, t), 0.3 (3H, s)	
[RhIr(CO)$_2$(η^2-HC≡CPh)(CCPh)(dppm)$_2$]-[O$_3$SCF$_3$] (**14**)[h]	22.5 (dm, $^1J_{RhP}$ = 101.1 Hz), −15.7 (m)		6.0 (1H, s), 4.1 (2H, m), 3.0 (2H, m)	
[RhIr(CO)$_2$(η^2-HC≡CCH$_3$)(CCPh)(dppm)$_2$]-[O$_3$SCF$_3$] (**15**)[h]	22.6 (dm, $^1J_{RhP}$ = 98.0 Hz), −13.5 (m)		3.9 (2H, m), 2.9 (2H, m), 1.9 (3H, s)	
[RhIr(CO)$_2$(η^2-PhC≡CPh)(CCPh)(dppm)$_2$]-[O$_3$SCF$_3$] (**16**)[h]	22.0 (dm, $^1J_{RhP}$ = 105.0 Hz), −15.5 (m)	193.5 (dt, Rh−*C*O, $^2J_{PC}$ = 15.7 Hz, $^1J_{RhC}$ = 81.2 Hz), 187.0 (t, Ir−*C*O, $^2J_{PC}$ = 7.1 Hz)	4.25 (2H, b), 3.1 (2H, b)	
[RhIr(CO)$_2$(CH$_3$OC(O)C≡CCO$_2$CH$_3$)-(CCPh)(dppm)$_2$][O$_3$SCF$_3$] (**17**)	19.6 (dm, $^1J_{RhP}$ = 107.6 Hz), −19.8 (m)	193.0 (dt, Rh−*C*O, $^2J_{PC}$ = 14.4 Hz, $^1J_{RhC}$ = 54.3 Hz), 178.8 (t, Ir−*C*O, $^2J_{PC}$ = 4.8 Hz)	4.1 (2H, m), 3.6 (2H, m), 2.7 (3H, s), 2.25 (3H, s)	2033(s), 1970(m), 1698(b,m)
[RhIr(CO)$_2$(μ-η^1-$\eta^{1'}$-CH$_3$OC(O)C≡CCO$_2$CH$_3$)-(CCPh)(dppm)$_2$][O$_3$SCF$_3$] (**18**)	6.62 (dm, $^1J_{RhP}$ = 89.0 Hz), −16.5 (m)	186.5 (dt, Rh−*C*O, $^2J_{PC}$ = 17.5 Hz, $^1J_{RhC}$ = 65.1 Hz), 175.0 (t, Ir−*C*O, $^2J_{PC}$ = 12.4 Hz), 176.5, 163.1 (s, *C*O$_2$CH$_3$), 116.2 (d, Ir−C≡*C*Ph, $^1J_{RhC}$ = 3.6 Hz), 109.4 (dt, Ir−*C*≡CPh, $^2J_{PC} \approx {}^1J_{RhC} \approx$ 5 Hz), 108.8 (dt, Rh−*C*(R)═CR, $^2J_{PC}$ = 9.2 Hz, $^1J_{RhC}$ = 23.1 Hz), 85.6 (dt, CR═*C*(R)−Ir, $^2J_{PC}$ = 14.6 Hz, $^1J_{RhC}$ = 7.2 Hz), 52.3, 51.8 (s, CO$_2$*C*H$_3$)	3.8 (3H, s), 2.6 (3H, s), 3.95 (2H, m), 3.65 (2H, m)	2034 (m), 2009 (s), 1699 (s)[l], 1592 (m)[k]
[RhIr(CO)$_2$(C≡CPh)(μ-H)(CCCH$_3$)(dppm)$_2$]-[O$_3$SCF$_3$] (**19**)	25.7 (dm, $^1J_{RhP}$ = 111.0 Hz), −21.1 (m)	192.3 (dt, Rh−*C*O, $^2J_{PC}$ = 15.3 Hz, $^1J_{RhC}$ = 80.8 Hz), 163.8 (dt, Ir−*C*O, $^2J_{PC} \approx {}^2J_{RhC} \approx$ 5.4 Hz), 89.2 (d, Ir−C≡*C*CH$_3$, $^1J_{RhC}$ = 4.7 Hz),[n] 53.0 (dtt, Ir−*C*≡CCH$_3$, $^1J_{RhC}$ = 4.6 Hz, $^2J_{P(Ir)C}$ = 8.1 Hz, $^2J_{P(Rh)C} \approx$ 4 Hz),[n] 69.1 (t, Ir−*C*≡CPh, $^2J_{PC}$ = 14.1 Hz), 110.9 (t, Ir−C≡*C*Ph, $^3J_{PC}$ = 2 Hz)	4.15 (m, 2H), 3.7 (m, 2H), 0.8 (s, 3H), −8.45 (m, 1H $^1J_{RhH} \approx$ 8.9 Hz, $^2J_{PH} \approx$ 8.9 Hz)	2129 (w),[k] 2078 (m), 2060 (w),[k] 1962 (s)
[RhIr(CO)$_2$(H)(μ-H)(CCPh)(dppm)$_2$]-[O$_3$SCF$_3$] (**21**)	24.8 (dm, $^1J_{RhP}$ = 105.0 Hz), −11.2 (m)	192.7 (dt, Rh−*C*O, $^2J_{PC}$ = 16.4 Hz, $^1J_{RhC}$ = 81.5 Hz), 167.0 (t, Ir−*C*O, $^2J_{PC} \approx$ 2 Hz), 70.1 (m, Ir−*C*≡CPh, $^1J_{RhC}$ = 5.2 Hz), 100.9 (d, Ir−C≡*C*Ph, $^1J_{RhC}$ = 4.6 Hz)	4.1 (m, 2H), 3.7 (m, 2H), −9.88 (dtt, $^1J_{RhH}$ = 16 Hz, $^2J_{PH}$ = 12 Hz, $^2J_{PH}$ = 5 Hz), −10.27 (dt, $^XJ_{RhH}$ = 2.2 Hz, $^2J_{PH}$ = 12.5 Hz)	1956(s), 2057(m)

[a] Abbreviations used: NMR, m = multiplet, dm = doublet of multiplets, s = singlet; d = doublet, t = triplet, q = quartet, dt = doublet of triplets, ddt = doublet of doublets of triplets, dtt = doublet of triplets of triplets, ddm = doublet of doublets of multiplets, b = broad; IR, w = weak, m = medium, s = strong, b = broad. [b] Vs 85% H_3PO_4 in CD_2Cl_2 at 25 °C unless otherwise stated. [c] Vs TMS in CD_2Cl_2 at 25 °C unless otherwise stated. [d] Nujol mull on KBr disks except compound **6** (THF solution in KCl cell), ν_{CO} unless otherwise noted. [e] −20 °C. [f] −40 °C. [g] −60 °C. [h] −80 °C. [i] −90 °C. [j] In THF-d^8. [k] $\nu_{C\equiv C}$. [l] ν_{CO} of ester. [m] ν_{SO}. [n] In the ^{13}C-enriched sample, $^1J_{CC}$ = 106.5 Hz.

in vacuo, leaving a red residue which was redissolved in a mixture of CH_2Cl_2 (10 mL) and THF (10 mL). Addition of pentane (55 mL) precipitated the product, which was washed with three 20-mL aliquots of pentane. The solid was dissolved in 10 mL of CH_2Cl_2 and 40 mL of THF, and the solution was refluxed for 2 h. The solvent was removed in vacuo, and the product was recrystallized from CH_2Cl_2/ether (10:60 mL). The red product was then washed three times with 10 mL aliquots of ether. Yield: 1.34 g (80%).

(c) Reaction of [RhIr(^{13}CO)$_2$(μ-η^1:$\eta^{2'}$-CCPh)(dppm)$_2$][O$_3$SCF$_3$] (2) with CO. An NMR tube was charged with compound **2** (20.0 mg, 14.6 μmol) containing ^{13}C-enriched carbonyl ligands and 0.4 mL of CD_2Cl_2. The sample was cooled to −80 °C in a dry ice−acetone bath, and an excess (≈2 mL, 80 μmol) of ^{12}CO was added via gastight syringe, causing a color change from red-purple to yellow. The ^{31}P{^{1}H} and ^{13}C-{^{1}H} NMR spectra of this sample, run at −80 °C, showed complete conversion of **2** to [RhIr(^{13}CO)(CO)(μ-η^1:$\eta^{2'}$-CCPh)(μ-^{13}CO)(dppm)$_2$][O$_3$SCF$_3$] (**1**), with the ^{12}C-carbonyl occupying the terminal position on iridium.

(d) Preparation of [RhIr(CO)$_2$(PMe$_3$)(μ-η^1:$\eta^{2'}$-CCPh)(dppm)$_2$][O$_3$SCF$_3$] (3). Compound **2** (20.7 mg, 15.1 μmol) was placed in a flask with 1 mL of CH_2Cl_2. Trimethylphosphine (1.6 μL, 15.5 μmol) was added via syringe, causing a color change from purple-red to orange. After the solution had stirred for 30 min, the orange product was precipitated by the addition of 10 mL of Et_2O. This was washed with three 5 mL aliquots of ether and then dried, first under nitrogen and then under vacuum. Yield: 14.7 mg (67%) Calcd for $C_{64}H_{58}O_5P_5RhIrF_3S$: C, 53.15; H, 4.04. Found: C, 52.89; H, 3.75.

(e) Preparation of [RhIr(CO)$_2$(PMe$_2$Ph)(μ-η^1:$\eta^{2'}$-CCPh)(dppm)$_2$][O$_3$SCF$_3$] (4). Compound **2** (90.6 mg, 66.1 μmol) was placed in a flask with 5 mL of THF. Phenyldimethylphosphine (9.5 μL, 66.8 μmol) was added via syringe, causing a color change from purple-red to brown, accompanied by the formation of a small amount of precipitate. After 30 min of stirring, 25 mL of ether was added to complete precipitation. The flocculent orange-brown solid was washed three times with 5 mL of ether and then dried, first under nitrogen and then under vacuum. Yield: 80.4 mg (81%) Calcd for $C_{69}H_{60}O_5P_5RhIrF_3S$: C, 54.95; H, 4.01. Found: C, 55.20; H, 3.87.

(f) Preparation of [RhIr(CO)$_2$(μ-SO$_2$)(μ-η^1:$\eta^{2'}$-CCPh)(dppm)$_2$][O$_3$SCF$_3$] (5). Compound **2** (30.7 mg, 22.4 μmol) was placed in a flask with 2 mL of THF, and an atmosphere of SO_2 was placed over the solution, resulting in a color change from red-purple to red-brown. After 15 min of stirring, 20 mL of ether was added, resulting in the formation of a flocculent orange precipitate. This was washed twice with 10 mL of ether. Yield: 12 mg (37%). Calcd for $C_{61}H_{49}P_4O_7S_2F_3RhIr$: C, 51.09; H, 3.44; S, 4.47. Found: C, 51.03; H, 3.07; S, 4.70.

(g) Reaction of [RhIr(CO)$_2$(μ-η^1:$\eta^{2'}$-CCPh)(dppm)$_2$][O$_3$SCF$_3$] with LiBH(Et)$_3$. An NMR tube was charged with compound **2** (20.1 mg, 14.7 μmol) and 0.5 mL of THF-d^8. The sample was cooled to −80 °C in a dry ice−acetone bath, and superhydride (1.0 M solution of LiBH(Et)$_3$ in THF; 15 μL, 15 μmol) was added via syringe, causing a color change to yellow brown. The NMR spectra at −60 °C showed complete conversion to **6a**. Further warming to −20 °C resulted in almost complete conversion to **6b**, along with a small quantity of **7a**. Warming the sample to room temperature caused it to change from brown to intense purple. The ^{31}P{^{1}H} NMR of this sample showed a mixture of **7a**,**b**.

(h) Preparation of [RhIr(CO)$_2$(μ-CCHPh)(dppm)$_2$] (7). A sample of compound **2** was dissolved in THF and cooled to −10 °C in a salt−ice bath. Superhydride (1 equiv) was added, and the solution was allowed to slowly warm to room temperature, causing a color change to intense purple. After the solution was stirred for 1 h at room temperature, the solvent was removed under a steady stream of nitrogen, and the purple solid was extracted into 5 mL of ether. This was filtered through Celite, and the solvent was removed under vacuum. No elemental analysis could be obtained for this compound, due to its high air-sensitivity.

(i) Preparation of [RhIr(CO)$_2$(η^2-CH$_2$=CH$_2$)(μ-η^1:$\eta^{2'}$-CCPh)(dppm)$_2$][O$_3$SCF$_3$] (8). An NMR tube was charged with compound **2** (18 mg, 13.1 μmol) and 0.4 mL of CD_2Cl_2. This was placed under an atmosphere of ethylene and cooled to −80 °C, causing a rapid color change to yellow. NMR spectroscopy showed complete conversion to **8**; however, ethylene was lost immediately upon warming, regenerating **2**.

(j) Preparation of [RhIr(CO)$_2$(η^2-CH$_2$=C=CH$_2$)(μ-η^1:$\eta^{2'}$-CCPh)(dppm)$_2$][O$_3$SCF$_3$] (9). An NMR tube was charged with compound **2** (18 mg, 13.1 μmol) and 0.4 mL of CD_2Cl_2. Allene was passed over this solution, causing a color change to yellow. The ^{1}H, ^{13}C{^{1}H}, and ^{31}P{^{1}H} NMR spectra of this solution at −30 °C showed complete conversion to a mixture of **9a**,**b**. This was not isolated in the solid state, due to facile loss of allene.

(k) Preparation of [RhIr(CO)$_2$(η^2-CH$_2$=C=C(CH$_3$)$_2$)(μ-η^1:$\eta^{2'}$-CCPh)(dppm)$_2$][O$_3$SCF$_3$] (10). A sample of compound **2** (75.0 mg, 54.7 μmol) was placed in a flask with 5 mL of CH_2Cl_2 and 5.4 μL (55.1 μmol) of dimethylallene, resulting in a color change from red-purple to orange. This was stirred for $^1/_2$ h and then precipitated by addition of 20 mL of pentane. The resulting orange microcrystalline solid was washed twice with 10 mL aliquots of pentane and dried under nitrogen. This compound was not dried under vacuum, due to facile loss of dimethylallene. The presence of 1 equiv of dichloromethane of crystallization was confirmed by elemental analysis and by X-ray structure determination. Yield: 73.9 mg (89%). Calcd for $C_{67}H_{59}O_5P_4RhIrF_3SCl_2$: C, 52.83; H, 3.90; Cl, 4.66. Found: C, 52.65; H, 3.59; Cl, 4.39.

(l) Preparation of [RhIr(CO)$_2$(η^2-CF$_3$C≡CCF$_3$)(μ-η^1:$\eta^{2'}$-CCPh)(dppm)$_2$][O$_3$SCF$_3$] (11). A sample of compound **2** (40.0 mg, 29.2 μmol) was placed in a flask and dissolved in 4 mL of THF. Hexafluoro-2-butyne was passed over the solution, resulting in a change from red-purple to orange-brown. After the solution was stirred for 1 h, the solvent was reduced to 2 mL under a steady stream of nitrogen, and the product precipitated by the addition of 15 mL of ether. The precipitate was washed twice with 10 mL of ether and dried under vacuum, giving a yellow microcrystalline powder. Yield: 30.5 mg (68%). Calcd for $C_{65}H_{49}O_5P_4RhIrF_9S$: C, 50.95; H, 3.22. Found: C, 50.85; H, 3.07.

(m) Preparation of [RhIr(CO)$_2$(η^2-CH$_3$O$_2$CC≡CCO$_2$CH$_3$)(μ-η^1:$\eta^{2'}$-CCPh)(dppm)$_2$][O$_3$SCF$_3$] (12). A sample of compound **2** (60 mg, 43.8 μmol) was placed in a flask and dissolved in 3 mL of CH_2Cl_2. This was cooled to 0 °C with an ice bath, and dimethyl acetylenedicarboxylate (DMAD) (5.6 μL, 45.6 μmol) was added via syringe. The resulting orange-brown solution was stirred for 30 min, and then 20 mL of ether was added. The resulting light brown powder was washed twice with 10 mL aliquots of ether and then dried, first under nitrogen and then under vacuum. Yield: 47.3 mg (71%). Calcd for $C_{67}H_{55}O_9P_4RhIrF_3S$: C, 53.25; H, 3.60. Found: C, 52.98; H, 3.49.

(n) Preparation of [RhIr(CO)$_2$(η^2-CH$_3$C≡CCO$_2$CH$_2$CH$_3$)(μ-η^1:$\eta^{2'}$-CCPh)(dppm)$_2$][O$_3$SCF$_3$] (13). An NMR tube was charged with compound **2** (17.4 mg, 12.7 μmol) and 0.5 mL of CD_2Cl_2, and ethyl 2-butynoate (1.5 μL, 12.9 μmol) was added. Cooling to −40 °C gave an orange solution which was shown by NMR spectroscopy to contain almost pure **13**. This solution reverted to **2** upon warming.

(o) Preparation of [RhIr(CO)$_2$(η^2-HC≡CPh)(μ-η^1:$\eta^{2'}$-CCPh)(dppm)$_2$][O$_3$SCF$_3$] (14). An NMR tube was charged with compound **2** (18.4 mg, 13.4 μmol) and 0.5 mL of CD_2Cl_2. The sample was cooled to −80 °C and treated with phenylacetylene (1.6 mL, 14.6 μmol), forming an orange solution. This solution was shown by NMR spectroscopy to contain pure **14**. Upon being warmed to −60 °C, this solution was converted

to a 2:1 mixture of **14**:**2**, and warming to −40 °C resulted in a 5:10:1 mixture of **14**, **2**, and the previously reported [RhIr(CO)$_2$(C≡CPh)(μ-H)(μ-η^1:$\eta^{2'}$-CCPh)(dppm)$_2$][O$_3$SCF$_3$][4g] (**19**). Further warming gave complete conversion to **19**.

(p) Preparation of [RhIr(CO)$_2$(η^2-HC≡CCH$_3$)(μ-η^1:$\eta^{2'}$-CCPh)(dppm)$_2$][O$_3$SCF$_3$] (15). An NMR tube was charged with compound **2** (14.6 mg, 10.7 μmol) and 0.5 mL of CD_2Cl_2. The sample was cooled to −80 °C and treated with propyne (450 μL, 18 μmol). This solution was shown by NMR spectroscopy to contain about 10% of compound **15**. Upon being warmed to −60 °C, this compound was converted to **2**, and warming to 25 °C resulted in formation of [RhIr(CO)$_2$(C≡CPh)(μ-H)(μ-η^1:$\eta^{2'}$-CCCH$_3$)(dppm)$_2$][O$_3$SCF$_3$] (**20**).

(q) Preparation of [RhIr(CO)$_2$(η^2-C$_6$H$_5$C≡CC$_6$H$_5$)(μ-η^1:$\eta^{2'}$-CCPh)(dppm)$_2$][O$_3$SCF$_3$] (16). An NMR tube was charged with compound **2** (19.7 mg, 14.4 μmol), 0.5 mL of CD_2Cl_2, and an excess of diphenylacetylene (5.0 mg, 28.1 μmol). Cooling this solution to −80 °C resulted in an orange-red solution which was shown by NMR to contain an 5:1 mixture of **16** and **2**. The diphenylacetylene ligand was lost upon warming, regenerating **2**.

(r) Preparation of [RhIr(CO)$_2$(CH$_3$O$_2$CC≡CCO$_2$CH$_3$)(μ-η^1:$\eta^{2'}$-CCPh)(dppm)$_2$][O$_3$SCF$_3$] (17). A sample of compound **2** (89.9 mg, 65.6 μmol) was placed in a flask and dissolved in 10 mL of CH_2Cl_2. DMAD (9.1 μL, 74.0 μmol) was added via syringe. The resulting orange-brown solution was stirred for 16 h, and then the solvent was reduced to 1 mL under a flow of nitrogen. A 20 mL volume of ether was added to precipitate the product, which was then recrystallized from 1 mL of CH_2Cl_2 and 20 mL ether, washed twice with 10 mL aliquots of ether, and dried under vacuum. Yield: 58 mg (58%).

(s) Preparation of [RhIr(CO)$_2$(μ-η^1:$\eta^{1'}$-CH$_3$O$_2$CC≡CCO$_2$CH$_3$)(μ-η^1:$\eta^{2'}$-CCPh)(dppm)$_2$][O$_3$SCF$_3$] (18). A sample of compound **2** (99.3 mg, 72.5 μmol) was placed in a flask and dissolved in 15 mL of THF. DMAD (8.9 μL, 72.4 μmol) was added via syringe, and the resulting yellow solution was heated to gentle reflux. After 1 h, the resulting red solution was reduced in volume to 5 mL and cooled to room temperature. Ether (15 mL) was added, causing the precipitation of **18** as an orange powder, which was washed twice with 10 mL aliquots of ether and dried under vacuum. Yield: 85 mg (78%). Calcd for C$_{67}$H$_{55}$O$_9$P$_4$RhIrF$_3$S: C, 53.25; H, 3.60. Found: C, 53.26; H, 3.73.

(t) Preparation of [RhIr(CO)$_2$(C≡CPh)(μ-H)(μ-η^1:$\eta^{2'}$-CCCH$_3$)(dppm)$_2$][O$_3$SCF$_3$] (20). A sample of **2** (40.6 mg, 29.6 μmol) was dissolved in 3 mL of THF and placed under 1 atm of propyne, causing a color change to brown. After the mixture was stirred for 1 h, 15 mL of pentane was added, giving a brown precipitate. This was redissolved in 1 mL of CH_2Cl_2 and precipitated by the addition of 10 mL of ether and 10 mL of pentane. The brown solid was washed twice with 10 mL of ether and dried. Yield: 29 mg (69%). Calcd for C$_{64}$H$_{53}$O$_5$P$_4$RhIrF$_3$S: C, 54.51; H, 3.79. Found: C, 54.31; H, 3.55.

(u) Preparation of [RhIr(CO)$_2$(H)(μ-η^1:$\eta^{2'}$-CCPh)(μ-H)(dppm)$_2$][O$_3$SCF$_3$] (21). A sample of **2** (40 mg, 29.2 μmol) was placed in a flask and dissolved in 3 mL of THF. Hydrogen gas was passed over the solution for 15 min, causing the solution color to change to brown. After 1 h of stirring, pentane (15 mL) was slowly added, giving a yellow microcrystalline precipitate. This was washed twice with 10 mL ether and dried under vacuum. Yield: 33.3 mg (83%). Calcd for C$_{61}$H$_{51}$O$_5$P$_4$RhIrF$_3$S: C, 53.40; H, 3.75. Found: C, 53.20; H, 3.54.

X-ray Data Collection. Suitable crystals of compound **10** were grown by slow diffusion of pentane into a concentrated CH_2Cl_2 solution of **10** (containing an excess of dimethylallene) at 22 °C. Data were collected to a maximum $2\theta = 50°$ on a Siemens P4/RA diffractometer using Mo Kα radiation at −60 °C. Unit cell parameters were obtained from a least-squares refinement of the setting angles of 54 reflections in the range $26.5° < 2\theta < 29.1°$. The cell parameters suggested either P1

Table 2. Crystallographic Experimental Details

A. Crystal Data	
formula	$C_{67}H_{59}Cl_2F_3IrO_5P_4RhS$
fw	1523.09
cryst dimens (mm)	0.65 × 0.56 × 0.17
cryst syst	triclinic
space group	$P\bar{1}$ (No. 2)
unit cell params[a]	
a (Å)	12.3608(11)
b (Å)	15.4205(15)
c (Å)	18.966(2)
α (deg)	107.709(7)
β (deg)	96.972(7)
γ (deg)	109.530(7)
V (Å^3)	3143.9(5)
Z	2
ρ_{calcd} (g cm^{-3})	1.609
μ (mm^{-1})	2.655
B. Data Collection and Refinement Conditions	
diffractometer	Siemens P4/RA[b]
radiation [λ (Å)]	graphite-monochromated Mo Kα (0.71073)
temp (°C)	−60
scan type	θ−2θ
data collcn 2θ limit (deg)	50.0
total no. of data collcd	10 949 (−13 ≤ h ≤ 14, −16 ≤ k ≤ 16, 0 ≤ l ≤ 22)
no. of indepdt reflns	10 612
no. of obs (NO)	9512 ($F_o^2 \geq 2\sigma(F_o^2)$)
structure solution method	direct methods (SHELXS-86[c])
refinement method	full-matrix least-squares on F^2 (SHELXL-93[d])
abs corr method	Gaussian integration (face-indexed)
range of transm factors	0.6752−0.4393
data/restraints/parameters	10553 [$F_o^2 \geq -3\sigma(F_o^2)$]/16[e]/799
goodness-of-fit (S)[f]	1.197 [$F_o^2 \geq -3\sigma(F_o^2)$]
final R indices[g]	
$F_o^2 > 2\sigma(F_o^2)$	$R_1 = 0.0514$, w$R_2 = 0.1313$
all data	$R_1 = 0.0612$, w$R_2 = 0.1505$
largest diff peak and hole (e Å^{-3})	3.130[h] and −0.950

[a] Obtained from least-squares refinement of 36 reflections with $26.6° < 2\theta < 29.1°$. [b] Programs for diffractometer operation and data collection were those of the XSCANS system supplied by Siemens. [c] Sheldrick, G. M. *Acta Crystallogr.* **1990**, *A46*, 467−473. [d] Sheldrick, G. M. SHELXL-93. Program for crystal structure determination. University of Göttingen, Germany, 1993. Refinement on F_o^2 for all reflections except for 59 having $F_o^2 < -3\sigma(F_o^2)$. Weighted R-factors wR_2 and all goodnesses of fit S are based on F_o^2; conventional R-factors R_1 are based on F_o, with F_o set to zero for negative F_o^2. The observed criterion of $F_o^2 > 2\sigma(F_o^2)$ is used only for calculating R_1 and is not relevant to the choice of reflections for refinement. R-factors based on F_o^2 are statistically about twice as large as those based on F_o, and R-factors based on *all* data will be even larger. [e] Restraints were applied to enforce idealized geometries within both positions of the disordered dichloromethane molecule (d(Cl(1)−C(103)) = d(Cl(2)−C(103)) = d(Cl(3)−C(104)) = d(Cl(4)−C(104)) = 1.80 Å; d(Cl(1)···Cl(2)) = d(Cl(3)···Cl(4)) = 2.95 Å) and one of the orientations of the CF$_3$ group of the disordered triflate anion (d(S(2)−C(102)) = 1.80 Å; d(F(104)−C(102)) = d(F(105)−C(102)) = d(F(106)−C(102)) = 1.35 Å; d(F(104)···F(105)) = d(F(104)···F(106)) = d(F(105)···F(106)) = 2.20 Å). Distance restraints were also applied to keep one of the dichloromethane "molecules" (the one containing Cl(1), Cl(2) and C(103)) in approximately the same region of space as one of the CF$_3$ group orientations (the one centered by C(102)): d(Cl(1)···S(2)) = 2.75 Å; d(Cl(2)···S(2)) = 3.65 Å; d(S(2)···C(103)) = 2.30 Å; d(C(102)···C(103)) = 0.90 Å (these distances were based on the corresponding Cl(3)···S(2), Cl(4)···S(1), S(1)···C(104) and C(101)···C(104) distances of the alternate triflate and dichloromethane orientations). [f] $S = [\sum w(F_o^2 - F_c^2)^2/(n-p)]^{1/2}$ (n = number of data; p = number of parameters varied; $w = [\sigma^2(F_o^2) + (0.0257P)^2 + 39.5280P]^{-1}$, where $P = [\mathrm{Max}(F_o^2, 0) + 2F_c^2]/3$). [g] $R_1 = \sum||F_o| - |F_c||/\sum|F_o|$; $wR_2 = [\sum w(F_o^2 - F_c^2)^2/\sum w(F_o^4)]^{1/2}$. [h] The largest residual peaks were found in the vicinity of the disordered triflate ion and dichloromethane molecule and were without chemical significance.

Table 3. Selected Interatomic Distances (Å)

Ir−Rh	2.8759(7)	P(1)−C(10)	1.828(8)
Ir−P(1)	2.351(2)	P(2)−C(10)	1.830(9)
Ir−P(3)	2.355(2)	P(3)−C(20)	1.827(8)
Ir−C(1)	1.984(9)	P(4)−C(20)	1.840(8)
Ir−C(3)	2.163(9)	O(1)−C(1)	1.153(10)
Ir−C(4)	2.049(8)	O(2)−C(2)	1.158(11)
Ir−C(8)	2.054(8)	C(3)−C(4)	1.433(12)
Rh−P(2)	2.329(2)	C(4)−C(5)	1.335(13)
Rh−P(4)	2.332(2)	C(5)−C(6)	1.497(14)
Rh−C(1)	2.374(9)	C(5)−C(7)	1.514(13)
Rh−C(2)	1.828(9)	C(8)−C(9)	1.218(12)
Rh−C(8)	2.271(8)	C(9)−C(91)	1.447(12)
Rh−C(9)	2.516(8)		

Table 4. Selected Interatomic Angles (deg)

Rh−Ir−P(1)	91.51(6)	P(4)−Rh−C(8)	89.2(2)
Rh−Ir−P(3)	90.73(5)	P(4)−Rh−C(9)	83.1(2)
Rh−Ir−C(1)	54.8(3)	C(1)−Rh−C(2)	105.6(4)
Rh−Ir−C(3)	161.4(2)	C(1)−Rh−C(8)	88.3(3)
Rh−Ir−C(4)	158.8(3)	C(1)−Rh−C(9)	116.9(3)
Rh−Ir−C(8)	51.6(2)	C(2)−Rh−C(8)	166.1(4)
P(1)−Ir−P(3)	177.50(8)	C(2)−Rh−C(9)	137.4(4)
P(1)−Ir−C(1)	90.0(2)	C(8)−Rh−C(9)	28.9(3)
P(1)−Ir−C(3)	90.7(2)	Ir−P(1)−C(10)	110.4(3)
P(1)−Ir−C(4)	88.3(3)	Rh−P(2)−C(10)	112.3(3)
P(1)−Ir−C(8)	91.7(2)	Ir−P(3)−C(20)	112.0(3)
P(3)−Ir−C(1)	92.2(2)	Rh−P(4)−C(20)	111.3(3)
P(3)−Ir−C(3)	87.5(2)	Ir−C(1)−Rh	82.1(3)
P(3)−Ir−C(4)	89.2(2)	Ir−C(1)−O(1)	155.1(8)
P(3)−Ir−C(8)	88.9(2)	Rh−C(1)−O(1)	122.8(7)
C(1)−Ir−C(3)	106.7(4)	Rh−C(2)−O(2)	178.7(10)
C(1)−Ir−C(4)	146.3(4)	Ir−C(3)−C(4)	65.9(5)
C(1)−Ir−C(8)	106.5(3)	Ir−C(4)−C(3)	74.5(5)
C(3)−Ir−C(4)	39.7(3)	Ir−C(4)−C(5)	143.4(7)
C(3)−Ir−C(8)	146.7(3)	C(3)−C(4)−C(5)	142.1(9)
C(4)−Ir−C(8)	107.2(3)	C(4)−C(5)−C(6)	123.9(9)
Ir−Rh−P(2)	92.34(6)	C(4)−C(5)−C(7)	120.2(9)
Ir−Rh−P(4)	93.51(6)	C(6)−C(5)−C(7)	115.9(9)
Ir−Rh−C(1)	43.1(2)	Ir−C(8)−Rh	83.2(3)
Ir−Rh−C(2)	148.6(3)	Ir−C(8)−C(9)	167.6(7)
Ir−Rh−C(8)	45.2(2)	Rh−C(8)−C(9)	86.8(6)
Ir−Rh−C(9)	73.9(2)	Rh−C(9)−C(8)	64.3(5)
P(2)−Rh−P(4)	169.81(8)	Rh−C(9)−C(91)	130.9(6)
P(2)−Rh−C(1)	94.1(2)	C(8)−C(9)−C(91)	161.7(9)
P(2)−Rh−C(2)	88.6(3)	P(1)−C(10)−P(2)	112.4(4)
P(2)−Rh−C(8)	89.0(2)	P(3)−C(20)−P(4)	112.6(4)
P(2)−Rh−C(9)	90.6(2)	C(9)−C(91)−C(92)	123.2(8)
P(4)−Rh−C(1)	95.9(2)	C(9)−C(91)−C(96)	117.8(8)
P(4)−Rh−C(2)	90.8(3)		

or $P\bar{1}$ space groups; successful solution and refinement of the structure confirmed $P\bar{1}$ to be the correct choice. Three reflections were chosen as intensity standards and were remeasured after every 200 reflections. There was no significant variation in the intensities of either set of standards, so no correction was applied. Absorption corrections were applied to the data. See Table 2 for a summary of crystal data and X-ray collection information.

The structure was solved by direct methods, using SHELXS-86 to locate the Ir, Rh, and P atoms. All other atoms were located after subsequent least-squares cycles and difference Fourier syntheses. Refinement was completed using the program SHELXS-93. All hydrogen atoms of the complex were included as fixed contributions; their idealized positions were generated from the geometries of the attached carbon atoms and their thermal parameters set at 20% greater than the isotropic thermal parameter of these carbons. The triflate anion and the dichloromethane solvent molecule were found to be disordered over a common region of space. Alternate orientations of the triflate ion were present in an approximate 50:50 occupancy ratio, with these orientations sharing two oxygen positions (O(101) and O(102)), with the two half-occupancy CH_2Cl_2 molecules superimposed on the triflate ion positions (specifically in the region of the triflate CF_3 group). All significant residual peaks on a final difference Fourier map were in the vicinity of this anion/solvent disorder.

The final model for the complex refined to values of $R_1 = 0.0514$ (for $F_o^2 \geq 2\sigma(F_o^2)$) and $wR_2 = 0.1505$ (on all data). Atomic coordinates and displacement parameters are given in the Supporting Information, and selected bond lengths and angles are given in Tables 3 and 4, respectively.

Results and Compound Characterization

The phenylacetylide-bridged, tricarbonyl complex $[RhIr(CO)_2(\mu\text{-}C_2Ph)(\mu\text{-}CO)(dppm)_2][O_3SCF_3]$ (**1**), although earlier obtained in our group by the reaction of the tricarbonyl methyl complex $[RhIr(CH_3)(CO)_3(dppm)_2][O_3SCF_3]$ with phenylacetylene,[4g] is more conveniently prepared as the chloride salt, via the trans-metalation method of Shaw,[12] in which the AgCl moiety is displaced from $[IrAgCl(C_2Ph)(CO)(dppm)_2]$ by a "$RhCl(CO)_2$" fragment. In all subsequent chemistry, the chloride ion is replaced by triflate in order to reduce the possibility of anion coordination. Compound **1** is labile and readily loses CO under reflux in CH_2Cl_2/THF to form $[RhIr(CO)_2(\mu\text{-}C_2Ph)(dppm)_2][O_3SCF_3]$ (**2**), a mixed-metal analogue of Grundy's alkynyl-bridged compounds, $[Rh_2(CO)_2(\mu\text{-}C_2R)(dppm)_2][ClO_4]$[15] (R = H, Ph, ^{t}Bu). Compound **2** is another member of a series of A-frame complexes containing an anionic ligand at the bridgehead position and terminal carbonyl groups.[4] Characterization of **2** is based on its NMR spectral parameters and on analogies with the structurally characterized $[Rh_2(CO)_2(\mu\text{-}C_2{}^tBu)(dppm)_2][ClO_4]$.[16] The $^{13}C\{^1H\}$ NMR spectrum displays two resonances in a region typical of terminal carbonyls (ca. δ 185), with only one of these displaying coupling to Rh (81.1 Hz). Furthermore, the IR spectrum shows two terminal carbonyl stretches. The alkynyl carbons are observed at δ 106.0 and 107.9 in the $^{13}C\{^1H\}$ NMR spectrum, and the latter is identified as the α-carbon, on the basis of the greater coupling to the Ir-bound phosphines. Both alkynyl carbons display almost equal coupling to Rh (5.1 and 5.7 Hz), consistent with the bonding mode in which the alkynyl group is σ-bound to Ir and side-on bound to Rh. In the alternate binding modes in which the alkynyl could be either symmetrically bridging the metals or σ-bound to Rh and π-bound to Ir, the Rh coupling to the α-carbon would be expected to be significantly greater than that to the β-carbon.

It has been shown that the dppm-bridged dirhodium alkynyl-bridged species,[15,16] along with the related species $[Rh_2(\mu\text{-}O_2CCH_3)(\mu\text{-}\eta^1{:}\eta^2\text{-}CCR)(CO)_2(PCy_3)_2]$,[8b] $[Rh_2(\mu\text{-}O_2CCH_3)(\mu\text{-}\eta^1{:}\eta^2\text{-}CCPh)(COD)_2]$,[8b] and $[NBu_4]_2[(C_6F_5)_2Pt(\mu\text{-}\eta^1{:}\eta^2\text{-}CCPh)(\mu\text{-}\eta^2{:}\eta^1\text{-}CCPh)Pt(C_6F_5)_2]$,[17] is fluxional, having the alkynyl group moving from one metal to the other in a "windshield-wiper" fashion. In contrast, the heterobinuclear species **2** is static, as was also reported for $[RhPtCl(\mu\text{-}CCCH_3)(CO)(dppm)_2][PF_6]$.[18] The $^{31}P\{^1H\}$ and $^{13}C\{^1H\}$ NMR spectra of **2** are essentially invariant from room temperature to −80 °C.

(15) Deraniyagala, S. P.; Grundy, K. R. *Organometallics* **1985**, *4*, 424.

(16) Loeb, S. J.; Cowie, M. *Organometallics* **1985**, *4*, 852.

(17) Forniés, J.; Lalinde, E. *J. Chem. Soc., Dalton Trans.* **1996**, 2587.

(18) Hutton, A. T.; Shehanzadeh, B.; Shaw, B. L. *J. Chem. Soc., Chem. Commun.* **1984**, 549.

Scheme 1

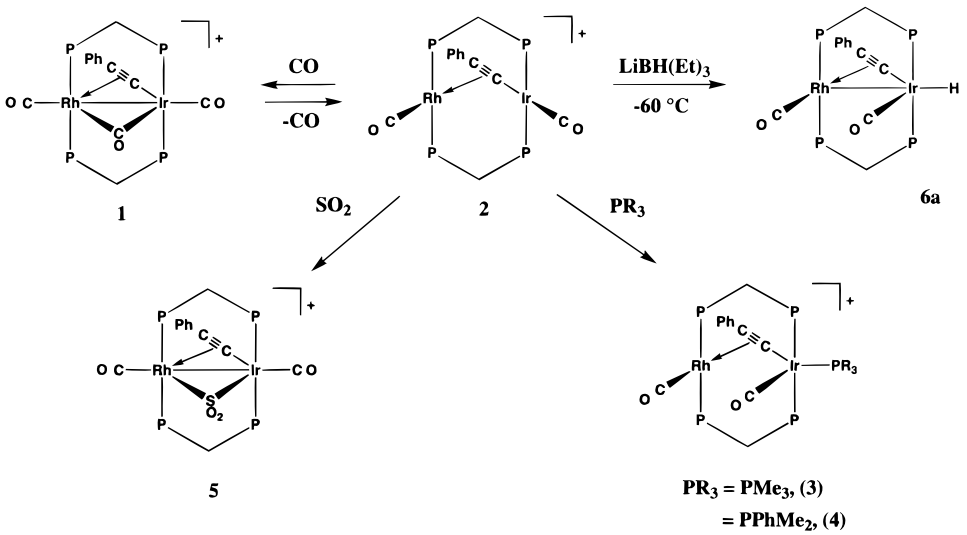

Compound **2** presents a number of different sites of attack for substrate molecules. As with other A-frame complexes having coordinative unsaturation at both metals, substrate attack can occur either on the inside (i.e. between the metals) or on the outside of the framework defined by the metals, the terminal carbonyls, and the bridging ligand, diagrammed (dppm ligands above and below the plane of the drawing are omitted) as follows:

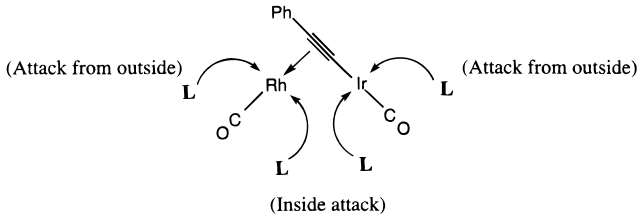

Furthermore, since the two metals differ, attack at rhodium will clearly be different from attack at iridium. In addition, substrate attack (either nucleophilic or electrophilic) can occur at the bridging alkynyl group. We therefore undertook an investigation of the reactivity of **2** with a number of substrates to determine the sites of reactivity in the molecule, with particular interest in inducing transformations of the alkynyl group.

Carbon monoxide attacks compound **2** at the external face of the A-frame, at iridium, giving compound **1** (Scheme 1). When ^{12}CO is placed over a solution of ^{13}CO-enriched **2** at low temperature (to inhibit rapid scrambling of the carbonyls), the ^{12}CO is found to occupy only the terminal position on iridium as shown by the $^{13}C\{^1H\}$ NMR spectrum, which shows only signals for the rhodium-bound and semibridging carbonyls, at δ 195.7 ($^1J_{RhC}$ = 80.0 Hz) and δ 198.7 ($^1J_{RhC}$ = 26.8 Hz), respectively, consistent with that reported for **1**.[4g]

Attack by PMe_3 and PMe_2Ph also appears to occur on the outside of the A-frame, at iridium, to give **3** and **4**, respectively, as shown in Scheme 1. Although the phosphorus nucleus of the PR_3 group couples to rhodium and to the rhodium-bound carbonyl, the rhodium coupling is quite small ($J_{RhP} \approx 7$ Hz), ruling out direct phosphine coordination to this metal. While the other possible isomer (resulting from attack of the phosphine from within the "pocket" of the A-frame) cannot be ruled out on the basis of the spectroscopy, the signal for the iridium-bound carbonyl in the $^{13}C\{^1H\}$ NMR spectrum of **4** (at δ 185.5) suggests that it is angled toward the rhodium, since, in these adducts of **2**, compounds in which the carbonyl is angled away from the rhodium have $^{13}C\{^1H\}$ NMR signals in the range δ 175−180, whereas carbonyls aimed between metals have lower-field chemical shifts, possibly resulting from a weak bridging interaction with the second metal. Coordination of the bulky phosphine inside the pocket of the A-frame also appears less likely due to unfavorable steric interactions involving the dppm phenyl groups. Coordination at iridium is expected for steric as well as electronic reasons; not only is coordination at rhodium disfavored owing to steric repulsion involving the phenyl substituent of the bridging C≡CPh group, but coordination at Ir is favored by the stronger Ir−P vs Rh−P bond. Compound **3** is isoelectronic with the carbonyl adduct (**1**) but differs in having only terminal carbonyl groups. It is assumed that the carbonyl group remains terminal on Ir to remove the excess electron density resulting from σ-donation by the two dppm groups and the PR_3 group (it should be recalled that the η^1-acetylide is a poor π-acceptor[11]). Compound **2** does not react with PPh_3, presumably owing to the bulk of this ligand.

The reaction of **2** with phosphines is in contrast to the reaction involving the dirhodium analogue $[Rh_2(CO)_2(\mu\text{-}C_2H)(dppm)_2][ClO_4]$,[15] which yielded phosphonium vinylidenes, in which the PR_3 group coordinated to the alkynyl β-carbon. This is certainly not the case for compounds **3** and **4**; for compound **4** the ^{13}C chemical shifts for C_α and C_β of the phenylacetylide group are inconsistent with those expected for a vinylidene (see compounds **7a**,**b** for example), and neither signal displays significant coupling to the high-field phosphorus nucleus, as would be expected for a phosphonium vinylidene. Although the failure of the phosphines to migrate from Ir to the alkynyl β-carbon, yielding a phosphonium vinylidene, may be a consequence of a stronger Ir−PR_3 bond, the presence of the bulky phenyl group on the alkynyl ligand of **2** would also be expected to inhibit such a migration of the sterically demanding PR_3 ligands.

Scheme 2

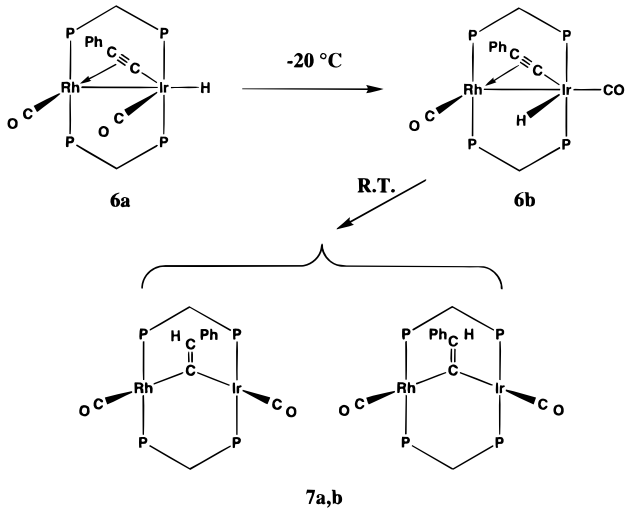

In contrast to the previous reactions, attack of **2** by SO_2 appears to occur on the inside of the A-frame, between the metals, yielding the SO_2-bridged [RhIr(CO)$_2$(μ-C$_2$Ph)(μ-SO$_2$)(dppm)$_2$][O$_3$SCF$_3$] (**5**). Spectral identification of the binding mode of the SO_2 ligand is not straightforward. While the ν_{SO} of 1213, 1174, 1063, and 1042 cm^{-1} in the IR spectrum are consistent with a bridging SO_2 group, these data are also consistent with terminal, pyramidal SO_2 binding,[19] as seen by the similarity of the SO stretches in **5** with those of the analogous mononuclear complex [Ir(CCPh)(CO)(PPh$_3$)$_2$(SO$_2$)] (ν_{SO} = 1196, 1181, 1050 cm^{-1}).[2b] However, the close similarity of the spectral parameters between **1** and **5** argues for analogous structures; furthermore, the presence of only terminal carbonyls in **5** and the known tendency for SO_2 to bridge two metals suggest the structure shown. It should also be noted that the high-field chemical shift for the Ir-bound carbonyl (δ 177.1) is consistent with the structure shown, as explained earlier.

Hydride attack on **2** also appears to occur on the "outside" of the complex at Ir, much as was observed with CO and phosphines, although at ambient temperature migration of the hydride ligand to the β-position of the alkynyl group occurs, yielding a vinylidene group. The first product, [RhIr(H)(CO)$_2$(μ-CCPh)(dppm)$_2$] (**6a**), observed at −60 °C, is shown in Scheme 1. On the basis of the ^{1}H and ^{13}C{^{1}H} NMR spectra, the hydride and one carbonyl ligand are shown to be terminally bound to Ir (showing strong coupling to the iridium-bound phosphines but none to rhodium) with one carbonyl bound to Rh (showing strong coupling to rhodium). This species is apparently static on the NMR time scale, but as the temperature is raised to −20 °C, rearrangement to another isomer (**6b**) occurs (see Scheme 2). This new isomer is related to **6a** by interchange of the hydride and carbonyl ligand on Ir. Again the rearrangement of the carbonyl from an "inside" to an "outside" site on iridium is accompanied by an upfield shift in the ^{13}C{^{1}H} NMR spectrum (see Table 1). Compound **6b** is fluxional such that the AA′BB′X pattern observed in the ^{31}P{^{1}H} NMR spectrum at −20 °C transforms to an ABCDX pattern, typical of four chemically inequivalent phosphorus nuclei (X represents Rh), when cooled to −80 °C. This type of fluxionality has been previously observed in related systems[4m] and has been attributed to a twisting of the complex around the Rh−Ir axis; apparently in the low-temperature limiting structure the P−Rh−P vector is staggered with respect to the P−Ir−P vector resulting in inequivalence of the two phosphorus nuclei on a given metal. These phosphorus nuclei become equivalent on a time average at higher temperatures by the twisting process.

At 0 °C transformation of **6b** to the two isomers of the intensely colored vinylidene-bridged species (**7a**,**b**) occurs. Both isomers display C$_\alpha$ for the vinylidene ligand as multiplets in the region (δ 245−250) that has been shown[9] to be typical for such species; the appearance of these signals rules out the possibility of hydride migration onto the α-carbon of the alkynyl to give either a parallel- or perpendicular-bound alkyne complex, since these complexes typically give ^{13}C NMR signals in the range δ 120−150 and 60−100,[4g,20] respectively. Unfortunately, the β-carbon resonances are not observed and are assumed to be obscured by those of the phenyl carbons. The appearance of both isomers is not surprising since rotation of vinylidenes about the C=C axis, both on single metal centers and when bridging metals, has been observed.[9] The ^{1}H NMR signal for the vinylidene hydrogen was not observed for either isomer and is presumably obscured by phenyl resonances which appear in the same region of the spectrum. As reported for the analogous dirhodium species,[15] compound **7** is very air-sensitive, oxidizing to an uncharacterized mixture of compounds (including approximately 20% of **2**) upon exposure to traces of air.

Compound **2** also reacts with ethylene at low temperatures, as shown in Scheme 3, forming the ethylene adduct [RhIr(CO)$_2$(C$_2$H$_4$)(μ-CCPh)(dppm)$_2$][O$_3$SCF$_3$] (**8**), in which the alkene is terminally bound to iridium, as is found in the compounds [Ir$_2$(CO)(C$_2$H$_4$)(μ-I)(μ-CO)(dppm)$_2$][X] (X = BF$_4$, I).[21] This adduct is very labile, however, and readily loses ethylene at temperatures higher than −40 °C. The characterization of **8** as having a terminally bound ethylene and a semibridging CO is based upon its NMR spectra. First, upon coordination of the alkene, the ^{31}P NMR signals for the rhodium-bound phosphines change only slightly, while those for the iridium-bound phosphines shift substantially upfield, suggesting that the site of coordination is at iridium. In the presence of a large excess of C$_2$H$_4$, raising the temperature from −50 °C causes the Ir-bound phosphorus resonance to broaden substantially, until at 0 °C it has disappeared into the baseline, offering additional support for reversible ethylene coordination at Ir. Although the signal for the iridium-bound carbonyl in the ^{13}C{^{1}H} NMR spectrum is broad and shows no discernible coupling to phosphorus or to rhodium, the chemical shift (δ 186.9) is consistent with the carbonyl being angled toward rhodium. The ^{1}H NMR signals for the ethylene hydrogens are in the expected range for an olefin complex; however, they are

(19) Kubas, G. J. *Inorg. Chem.* **1979**, *18*, 182.

(20) (a) Xiao, J.; Cowie, M. *Organometallics* **1993**, *12*, 463 (b) Wang, L.-S.; Cowie, M. *Organometallics* **1995**, *14*, 2374. (c) Wang, L.-S.; Cowie, M. *Organometallics* **1995**, *14*, 3040. (d) Wang, L.-S.; Cowie, M. *Can. J. Chem.* **1995**, *73*, 1058.

(21) Vaartstra, B. A.; Xiao, J.; Jenkins, J. A.; Verhagen, R.; Cowie, M. *Organometallics* **1991**, *10*, 2708.

Scheme 3

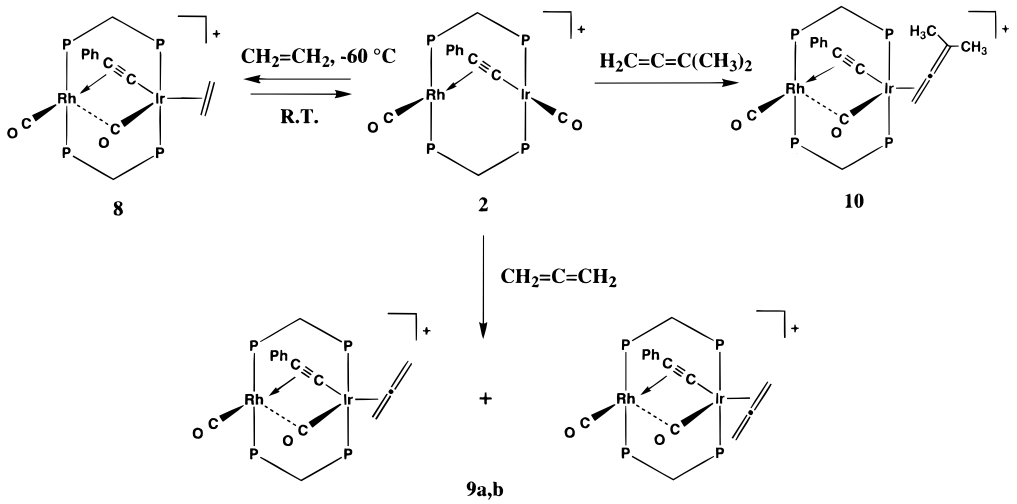

broad and show no coupling, giving little useful structural information. Finally, the $^{13}C\{^1H\}$ and $^{31}P\{^1H\}$ NMR spectra of this complex are very similar to the structurally characterized dimethylallene adduct **10** (vide infra), which is shown to have the alkene bound to iridium, on the "outside" of the complex.

More stable olefin adducts can be formed by the use of cumulated alkenes. Allene reacts with **2** to give a mixture of two isomers, which were identified on the basis of their NMR spectra. These isomers are diagrammed in the plane of the "$RhIr(C_3H_4)$" moiety (dppm ligands omitted), showing their relationship. While the spectral data available are insufficient to unambiguously assign the two geometries to the two isomers, the major isomer has been given the designation **9a**. The

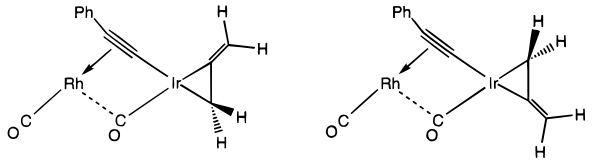

9a, b

$^{13}C\{^1H\}$ NMR signals for the iridium-bound carbonyls of both isomers appear in the same region, and one isomer shows coupling to rhodium (5 Hz) as expected for a semibridging interaction (the signal for the carbonyl of **9b** is broad and unresolved). These isomers exchange rapidly at room temperature, showing very broad signals in the ^1H and $^{31}P\{^1H\}$ NMR spectra. While it was initially thought that the mechanism of this exchange might involve either an "allene roll"[22] or allene rotation about the Ir−olefin bond, spin saturation transfer NMR experiments at 0 °C showed that the dominant exchange pathway was between the coordinated and free allene molecules, indicating a dissociative mechanism. Exchange could not be observed by this experiment at −20 °C. The presence of two isomers of this sort is similar to that found in the isoelectronic $[Ir_2(CO)_2(\eta^2\text{-}C_3H_4)(\mu\text{-}I)(dppm)_2][O_3SCF_3]$.[4e]

The substituted cumulene, 1,1-dimethylallene, reacts with **2** to form **10**, which is more stable than the unsubstituted allene adduct, consistent with observations in other systems.[23] The methyl substituents on the allene also increase the bulkiness of one end of the ligand, so that only one isomer is sterically favorable, having the noncoordinated double bond of the allene cis to the alkynyl ligand. This compound was characterized by an X-ray structure determination and has the structure shown in Figure 1. The $^{13}C\{^1H\}$ NMR spectrum of this compound clearly shows the weak (6.3 Hz) coupling of the iridium-bound carbonyl to rhodium, indicating a semibridging interaction—a conclusion that is supported by the IR spectrum (ν_{CO} = 1882 cm^{-1}) and the X-ray structure.

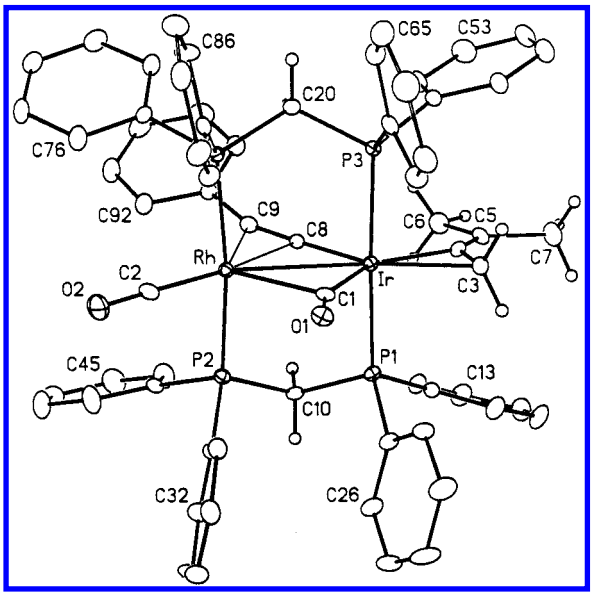

Figure 1. Perspective view of the $[RhIr(CO)(\eta^2\text{-}H_2C{=}C\text{-}CMe_2)(\mu\text{-}CO)(\mu\text{:}\eta^1,\eta^2\text{-}CCPh)(dppm)_2]^+$ complex cation showing the atom-labeling scheme. Non-hydrogen atoms are represented by Gaussian ellipsoids at the 20% probability level. Hydrogen atoms are shown with arbitrarily small thermal parameters for the dimethylallene and dppm methylene groups and are not shown for the phenyl groups.

The X-ray structure determination of **10** confirms the geometry proposed for all olefin adducts of **2** having the

(22) Foxman, B.; Marten, D.; Rosan, A.; Raghu, S.; Rosenblum, M. *J. Am. Chem. Soc.* **1977**, *99*, 2160.

(23) (a) Cooper, D. G.; Powell, J. *Inorg. Chem.* **1976**, *15*, 1959. (b) Hughes, R. P.; Powell, J. *J. Organomet. Chem.* **1973**, *60*, 409.

Scheme 4

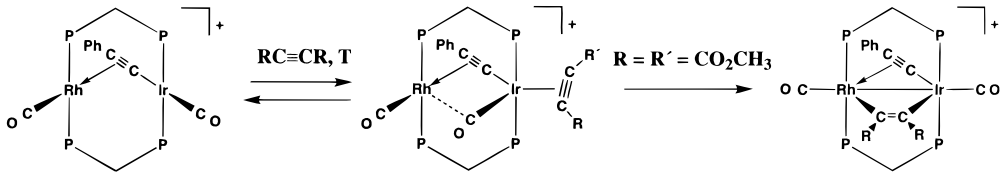

R = R´ = CF_3; 11 (T = 20 °C)

R = R´ = CO_2CH_3; 12 (T = 20 °C)

R = CH_3, R´ = $CO_2CH_2CH_3$; 13 (T = -40 °C)

R = Ph, R´ = H; 14 (T = -60 °C)

R = CH_3, R´ = H; 15 (T = -80 °C)

R = R´ = Ph; 16 (T = -80 °C)

olefin coordinated terminally to Ir. The dimethylallene moiety is coordinated through the unsubstituted end of the molecule with the methyl substituents on the side of the complex adjacent to the bridging alkynyl group and away from the semibridging carbonyl. Coordination to Ir has resulted in the expected lengthening of the C(3)−C(4) bond to 1.433(12) Å, compared to the uncomplexed C(4)−C(5) bond of 1.335(13) Å, and bending back of the olefinic moiety (C(3)−C(4)−C(5) = 142.1(9)°). The rhodium−alkynyl distances of 2.271(8) Å (to C_α) and 2.516(8) Å (to C_β) compare well to those found in the related compounds [RhIr(CCPh)(μ-CCPh)(μ-H)$(CO)_2$-$(dppm)_2$][O_3SCF_3] (**19**) (2.228(6) and 2.515(7) Å),[4g] [RhPt-$(dppm)_2$(CO)$(CCCH_3)$Cl][PF_6] (2.22(2) and 2.46(3) Å),[18] and [$Rh_2(CO)_2$(μ-CC^{t}Bu)$(dppm)_2$][ClO_4] (2.209(6) and 2.616(6) Å).[16] Further evidence for the binding of the alkynyl ligand to rhodium is found in the Ir−C(8)−C(9) angle of 167.6(7)°, in which the alkynyl group is pulled toward the rhodium. At C(9) the phenyl substituent is bent back away from the Rh as expected from the π-back-donation to this group. The much shorter rhodium−iridium distance in **10** (2.8759(7) Å) than in the related **19** (Rh−Ir 3.0582(8) Å[4g] is likely due to the presence of the semibridging carbonyl in **10**, which pulls the metals closer together, and the absence of a bridging hydride, which tends to lengthen the metal−metal separation.

The semibridging carbonyl interaction is characterized by the substantially shorter Ir−C(1) vs Rh−C(1) distance (1.984(9) Å vs 2.374(9) Å) and by the more linear carbonyl angle involving Ir (Ir−C(1)−O(1) = 155.1(8)°) than Rh (Rh−C(1)−O(1) = 122.8(7)°). As an aside, it should be noted that both dppm methylene groups are bent toward the bridging alkynyl group, thereby allowing phenyl groups 2, 3, 6, and 8, which are thrust into the region between the equatorial ligands, to avoid the bulky phenylacetylide and the methyl substituents on the dimethylallene ligand; if either of these methylene groups were to bend in the other direction, either phenyl groups 1 and 4 or phenyl groups 5 and 7 would be thrust into the vicinities of these methyl and phenyl substituents.

Compound **2** also reacts with a range of alkynes to yield complexes of varying stability (see Scheme 4). Complexes with electron-rich alkynes are unstable toward loss of the alkyne ligand except at very low temperatures. Increasing the π-acidity of the alkyne by the addition of electron-withdrawing groups results in much stronger coordination of the alkyne. Thus, while compound **2** does not completely react with an excess of propyne or diphenylacetylene (to form compounds **15** and **16**, respectively) at temperatures as low as −80 °C, the adduct of ethyl 2-butynoate (**13**) only loses the alkyne ligand at temperatures above −20 °C, and strongly electron-withdrawing alkynes, hexafluorobutyne (HFB) and dimethyl acetylenedicarboxylate (DMAD), give complexes (**11** and **12**) which are stable toward ligand loss at room temperature.

The structural similarity of these complexes, both to each other and to the alkene complexes, can be seen by their IR and NMR spectra, which differ only slightly with the identity of the ligands used. All show the iridium-bound phosphines in the $^{31}P\{^1H\}$ NMR spectra to be shielded by similar amounts by the presence of the additional ligand, with the phosphines on rhodium being only slightly affected by the added ligand. The iridium-bound carbonyl, in almost all cases, appears in the $^{13}C\{^1H\}$ NMR spectra slightly downfield from the starting material, with small coupling (<15 Hz) to Rh, indicating a semibridging geometry. For compounds **11** and **12**, a carbonyl stretch appears in the IR spectra in the 1860−1890 cm^{-1} region, consistent with a semibridging carbonyl. It is interesting to note that, in contrast to the allene adduct **9**, only one isomer is seen for the unsymmetric alkynes PhC≡CH and $CH_3C{\equiv}CCO_2CH_2$-CH_3. This is presumably due to the same steric effects which permit only one isomer for the substituted allene adduct **10**.

The hexafluorobutyne complex (**11**) is particularly informative, owing to the additional ^{19}F NMR data which show the trifluoromethyl signals as multiplets at δ −52.59 and −52.67. Decoupling the iridium-bound phosphines causes these multiplets to simplify to quartets ($^5J_{FF}$ = 3.65 Hz), while decoupling the rhodium-bound phosphines has no effect. This further suggests that the alkyne is bound only to iridium. The $^{13}C\{^1H\}$ NMR signals for the alkyne carbons (δ 92.9, 89.1) are also consistent with the proposed structure. Complex **11** is also spectroscopically similar to the related complex [RhIr(CO)(HFB)(μ-S)(μ-CO)$(dppm)_2$] and to [Ir_2-(CO)(HFB)(μ-S)(μ-CO)$(dppm)_2$], the latter of which was shown by X-ray crystallography to have a structure very similar to that proposed for **11**.[24] Surprisingly perhaps, the HFB ligand is more labile in the sulfido-bridged product than in **11**.[24] We had expected that the π-acidic HFB would coordinate more strongly to the electron-

(24) Vaartstra, B. A.; Cowie, M. *Organometallics* **1989**, *8*, 2388.

Scheme 5

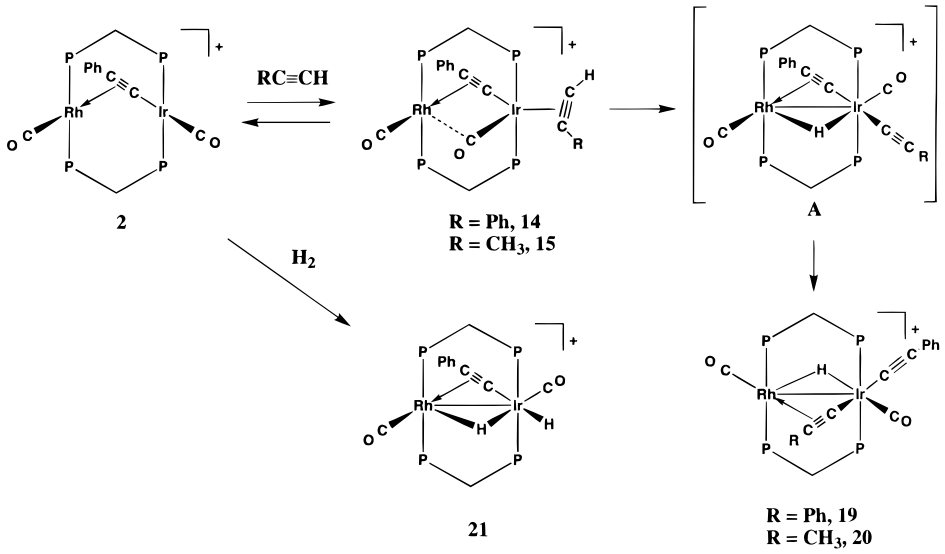

rich $[RhIr(CO)_2(\mu\text{-}S)(dppm)_2]$, for which the carbonyl stretches are at unusually low wavenumbers (ν_{CO}: 1932, 1906 cm^{-1}).[25]

The DMAD complex **12** differs from the other alkyne adducts in that it is unstable toward rearrangement. Upon standing in solution, **12** converts to complex **18**, having the DMAD ligand bridging the two metals in a parallel fashion. This is shown by the infrared spectrum of this compound, which shows $\nu_{C=C}$ = 1592 cm^{-1}, typical of an alkyne in this coordination mode, and the $^{13}C\{^1H\}$ NMR spectrum, which shows inequivalent alkyne carbons, each having substantially different coupling to the rhodium (23.1 Hz vs 7.2 Hz) and to the phosphine ligands. This spectrum also suggests that the phenylacetylide ligand is in its usual bridging position, as shown by the coupling to rhodium (3−5 Hz) of both alkynyl carbons. In addition, both carbonyls are clearly terminal, as shown by their signals in the $^{13}C\{^1H\}$ NMR spectrum (as each carbonyl shows coupling to only one set of phosphines, and only one shows coupling to rhodium) and the IR spectrum (ν_{CO} = 2034, 2009 cm^{-1}).

In the rearrangement of **12** to **18**, an intermediate isomer **17** is observed. Unfortunately, the resonances of the alkyne could not be located in the $^{13}C\{^1H\}$ NMR spectrum, and further characterization was not possible owing to its facile conversion to **18** even at low temperatures. This rearrangement is paralleled by the analogous reaction of $[RhIr(CO)_2(\mu\text{-}I)(dppm)_2][BF_4]$ with DMAD,[21] which also goes through at least one uncharacterized intermediate before yielding the alkyne-bridged complex $[[RhIr(CO)_2(\mu\text{-}I)(\mu\text{-}DMAD)(dppm)_2][BF_4]$. The hexafluorobutyne adduct **11** does not rearrange upon standing or with gentle reflux in dichloromethane and slowly converts to **2** upon reflux in THF, through dissociation of the alkyne. It is expected that HFB would form a more stable complex with **2**, due to its greater π-acidity,[26] so it remains unclear as to why the DMAD adduct rearranges to the alkyne-bridged species while HFB loss occurs in **11**.

Terminal alkynes, such as phenylacetylene or propyne, react with **2**, as shown in Scheme 5, to first give the adducts **14** and **15**, analogous to the HFB and DMAD adducts (**11** and **12**). However, these rearrange to the oxidative-addition products $[RhIr(CCPh)(CO)_2(\mu\text{-}H)(\mu\text{-}CCR)(dppm)_2][O_3SCF_3]$ (**19**, R = Ph; **20**, R = CH_3), of which the bis(phenylacetylide) **19** was previously reported in the reaction of $[RhIr(CH_3)(CO)_3(dppm)_2][O_3SCF_3]$ with excess phenylacetylene and was characterized crystallographically.[4g] The mixed bis(alkynyl) **20** shows very similar spectral characteristics, both in the IR and the NMR spectra, to the bis(phenylacetylide) complex and is assumed to have an analogous structure. Both complexes, for example, show a signal for the bridging hydride in the ^1H NMR spectrum near δ −8, showing comparable coupling (≈9 Hz) to the iridium-bound phosphines and to rhodium, as well as weaker coupling to the rhodium-bound phosphines.

Oxidative addition of propyne to compound **2** can result in two possible isomers: one in which the propynyl is terminal, while the phenylacetylide bridges the metals, and one in which the phenylacetylide is terminal and the propynyl ligand occupies the bridging position. Addition of ^{13}C-labeled propyne to **2** shows that only the second isomer is observed, having the propynyl ligand in the bridging position, with both the C_α and C_β nuclei showing coupling (4.6 and 4.7 Hz, respectively) to rhodium. The signals for the phenylacetylide carbons in the natural-abundance $^{13}C\{^1H\}$ NMR spectrum show no coupling to rhodium.

Reaction of **2** with dihydrogen also results in oxidative addition, giving $[RhIr(H)(CO)_2(\mu\text{-}CCPh)(\mu\text{-}H)(dppm)_2][O_3SCF_3]$ (**21**), much as was observed in dihydrogen addition to $[RhIr(CO)_2(\mu\text{-}Cl)(dppm)_2][BF_4]$ and $[RhIr(CO)_2(\mu\text{-}S)(dppm)_2]$.[25] The hydride ligands are believed to be mutually cis, with no H−H coupling seen in the $^1H\{^{31}P\}$ NMR spectrum. The alkynyl ligand remains in the bridging position, as indicated by the coupling to rhodium seen in both alkynyl carbon signals in the $^{13}C\{^1H\}$ NMR spectrum.

Unlike the neutral monohydride **6**, compound **21** does not rearrange to form a vinylidene upon warming;

(25) Vaartstra, B. A.; Cowie, M. *Inorg. Chem.* **1989**, *28*, 3138.
(26) Kosower, E. M. *An Introduction to Physical Chemistry*; Wiley: New York, 1968; p 49.

instead, dihydrogen elimination occurs upon heating, regenerating **2** (along with some of the previously characterized[27] complex $[RhIr(H)(CO)_2(\mu\text{-}H)_2(dppm)_2]^+$, from reaction with excess hydrogen and loss of phenylacetylene). Compound **21** can also be formed from addition of strong acid to compound **6a** at −80 °C. Deprotonation of **21** with strong base (KO^{t}Bu) at room temperature yields the vinylidene **7**, presumably through initial formation of **6b**.

Discussion

The A-frame complex $[RhIr(CO)_2(\mu\text{-}CCPh)(dppm)_2][O_3SCF_3]$ (**2**) is structurally analogous to the homobinuclear species $[Rh_2(CO)_2(\mu\text{-}CCR)(dppm)_2][ClO_4]$ (R = H, Ph, ^{t}Bu),[15] having the alkynyl group in an unsymmetrical, σ,π-binding mode. However, unlike the dirhodium analogues, the mixed-metal RhIr species is *not* fluxional but instead has the phenylacetylide group static and σ-bound to iridium and π-bound to rhodium. In the dirhodium system, the alkynyl group was found to move from one metal to the other in a windshield-wiper motion. The failure of **2** to rearrange to a species in which the alkynyl group is σ-bound to rhodium and π-bound to iridium presumably results from the lower stability of such a species, owing to the weaker Rh−C vs Ir−C σ bond.

As alluded to earlier, A-frame complexes such as **2** have two substantially different sites for substrate attack: either inside the A-frame pocket, between the metals, or outside this pocket, at a single metal site remote from the adjacent metal. When the two metals are also different, as in **2**, each of the inside or outside sites can also be differentiated by the different metal. With the exception of SO_2 and H_2, initial attack on **2** by all substrates investigated occurs on the outside of the complex at iridium; even if subsequent rearrangement occurs, an initial adduct having the substrate bound at the outside site on Ir is observed. We suggest that the preference for an outside site is based on less steric crowding in this position, whereas the preference for iridium is thermodynamic and based on stronger Ir−substrate bonds. It is not clear why SO_2 and H_2 apparently attack inside the pocket of the A-frame, between the metals. Although we cannot rule out outside attack followed by a facile rearrangement such that the initial adduct has too short a lifetime to be observed, we argue against this since all other substrates investigated show the adduct prior to rearrangement. This dichotomy of SO_2 attack at a site in the A-frame pocket while other substrates attack the outside site has been previously proposed,[28] and H_2 attack has previously been observed in the A-frame pocket in related compounds.[25]

In addition to the coordination sites at the metal, electrophilic or nucleophilic attack can also occur at the bridging alkynyl group (either at the α- or β-carbons). The dirhodium analogue $[Rh_2(CO)_2(\mu\text{-}CCH)(dppm)_2][ClO_4]$, for example, is reported to undergo attack by hydride and by phosphines to give the vinylidene-bridged products resulting from coordination of these nucleophiles at the acetylide β-carbon.[15] It is not known

Scheme 6

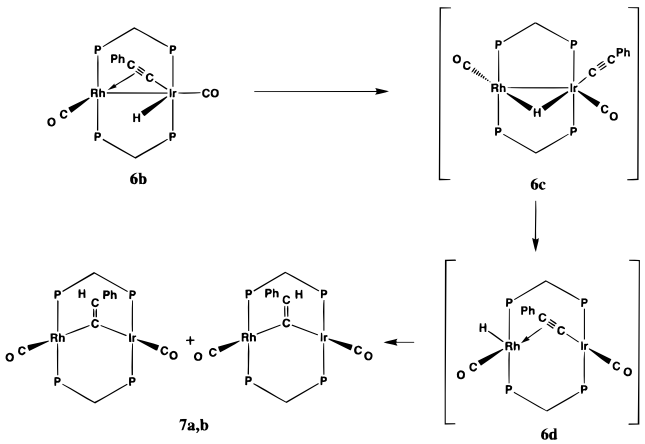

whether the acetylide group is the initial target or whether attack at a metal occurs with subsequent rearrangement. In the case of the RhIr complex **2**, attack by either H^- or PR_3 initially occurs at iridium, to give $[RhIr(H)(CO)_2(\mu\text{-}CCPh)(dppm)_2]$ (**6a**) or $[RhIr(PR_3)(CO)_2(\mu\text{-}CCPh)(dppm)_2][O_3SCF_3]$ ($PR_3 = PMe_3$ (**3**), $PPhMe_2$ (**4**)). The subsequent rearrangement of **6a** to the phenylvinylidene-bridged $[RhIr(CO)_2(\mu\text{-}CCHPh)(dppm)_2]$ (**7**) suggests a similar route for the dirhodium system, although we would expect this rearrangement to be more facile owing to the greater lability of rhodium compared to iridium. The failure of the phosphine adducts (**3**, **4**) to rearrange to the phosphonium−vinylidene analogues may result from steric interactions involving the bulky phenyl substituent on the phenylacetylide and the large phosphine ligands. In addition, the stronger Ir−PR_3 bond would inhibit such a migration.

Rearrangement of the hydride−phenylacetylide complex **6a** to the phenylvinylidene-bridged **7** proceeds via the isomeric hydride **6b**, which has resulted from interchange of the hydride and Ir-bound carbonyl position, such that the hydride ligand is now in the A-frame pocket. In Scheme 6 we propose a mechanism for rearrangement of **6b** to **7**. We believe that a pivotal intermediate in this rearrangement is the species diagrammed as **6d**, in which the hydride ligand is adjacent to the alkynyl β-carbon, facilitating migration to this carbon. We suggest that this intermediate, in which the hydride ligand is on the same face of the complex as the alkynyl group, results from **6b** by movement of the hydride between the metals. This can occur by replacement of the π interaction of the alkynyl with rhodium by a bridging hydride interaction (**6c**); this latter interaction maintains the electron count at each metal, since the hydride bridge can be viewed as an agostic interaction of the Ir−H bond with Rh. Having the hydride-bridged intermediate **6c**, twisting of the equatorial ligand framework about the metal−phosphine bonds brings the hydride between the metals, as has been proposed in a number of related systems.[27,29] Movement of the alkynyl group back to the bridging site, displacing the hydride bridge, generates **6d**, which has

(27) McDonald, R.; Cowie, M. *Inorg. Chem.* **1990**, *29*, 1564.
(28) (a) Cowie, M. *Inorg. Chem.* **1979**, *18*, 286. (b) Mague, J. T.; Sanger, A. R. *Inorg. Chem.* **1979**, *18*, 2060.
(29) (a) Puddephatt, R. J.; Azam, K. A.; Hill, R. H.; Brown, M. P.; Nelson, C. D.; Moulding, R. P.; Seddon, K. R.; Grossel, M. C. *J. Am. Chem. Soc.* **1983**, *105*, 5642. (b) Antonelli, D. M.; Cowie, M. *Organometallics* **1990**, *9*, 1818. (c) Antonelli, D. M.; Cowie, M. *Inorg. Chem.* **1990**, *29*, 4039.

an ideal structure to facilitate transfer of the hydride to the β-carbon of the phenylacetylide. A similar mechanism has been proposed for the formation of vinylidenes from related diiridium alkynyl−hydride complexes.[4g]

The DMAD adduct $[RhIr(CO)_2(DMAD)(\mu\text{-}CCPh)(dppm)_2][O_3SCF_3]$ (**12**), having the DMAD ligand bound on the outside of the complex at Ir (see Scheme 4), also rearranges in a manner not unlike that of **6a** to give the isomeric structure **18** in which the alkyne now bridges the metals opposite the bridging alkynyl group. This rearrangement is not unexpected since most other binuclear alkyne complexes have the alkyne in bridging sites.[20] The failure of the analogous alkyne adducts (**13**−**16** and particularly the closely related HFB complex **11**) to rearrange presumably results from their weaker binding which instead favors alkyne dissociation. In the rearrangement of **12** to **18** an intermediate **17** was observed; however, not enough spectral data were accessible to allow us to establish its structure so the mechanism of this rearrangement remains equivocal.

The reaction of **2** with terminal alkynes, as shown in Scheme 5, incorporates a number of the rearrangements proposed for other substrates. The first products have the alkyne bound on the outside of the complex at Ir, analogous to all initial olefin and alkyne adducts. We then propose a rearrangement (either as for the DMAD adduct rearrangement of **12** to **18** or via alkyne dissociation and recoordination) to a species having the alkyne on the inside of the complex, on Ir but adjacent to Rh. Oxidative addition would yield the hydride-bridged bis(acetylide) intermediate **A**, in which the phenylacetylide group has remained in the bridging site. This species rearranges to **20** in the propyne reaction, having the propynyl group in the bridging position and the phenylacetylide terminally bound to iridium. Although it would appear that **19** and **20** should be fluxional, via facile exchange of the terminal and bridging alkynyl groups, there is no evidence of this.

Concluding Remarks

The sites of attack by a number of small molecules on the phenylacetylide-bridged A-frame, $[RhIr(CO)_2(\mu\text{-}CCPh)(dppm)_2]^+$, have been determined. In most cases the initially observed species have the added ligand terminally bound to Ir on the "outside" of the A-frame structure, remote from Rh. Only H_2 and SO_2 are exceptions, with both apparently attacking in the A-frame pocket between the metals. Although one of our goals was to effect transformation of the acetylide group, this has only been achieved in the present study with the hydride group, in which hydride migration from Ir to the β-carbon of the acetylide occurred yielding a bridging phenylvinylidene group. A subsequent paper will describe extensions of the above chemistry, in which C−C bond formation, involving allyl group migration to the β-carbon of the acetylide group, is observed.[30]

Acknowledgment. We thank the Natural Sciences and Engineering Research Council of Canada (NSERC) and the University of Alberta for financial support of the research and the NSERC for funding the P4/RA diffractometer. We also thank Dr. J. M. Stryker for a loan of ^{13}C-labeled propyne.

Supporting Information Available: Tables of X-ray experimental details, atomic coordinates, interatomic distances, interatomic angles, anisotropic thermal parameters, and hydrogen parameters for compound **10** (15 pages). Ordering information is given on any current masthead page.

OM970946Q

(30) George, D. S. A.; McDonald, R.; Cowie, M. Manuscript in preparation.